Distribution of modern dinocysts and pollen in the western Mediterranean Sea (Algerian margin and Gulf of Lion)

V. Coussin, A. Penaud, N. Combourieu-Nebout, O. Peyron, Sabine Schmidt, Sebastien Zaragosi, A. de Vernal, N. Babonneau

Marine Micropaleontology
August 2022, Volume 175 Pages 102157 (20p.)
https://doi.org/10.1016/j.marmicro.2022.102157
https://archimer.ifremer.fr/doc/00791/90269/

Distribution of modern dinocysts and pollen in the western Mediterranean Sea (Algerian margin and Gulf of Lion)

Coussin Vincent [1, *], Penaud A. [1], Combourieu-Nebout N. [2], Peyron O. [3], Schmidt S. [4], Zaragosi S. [4], De Vernal A. [5], Babonneau Nathalie [1]

[1] Univ. Brest, CNRS, Ifremer, Geo-Ocean, UMR 6538, F-29280 Plouzané, France
[2] HNHP, CNRS, UMR 7194, Département de Préhistoire du Muséum d'Histoire Naturelle, F-75013 Paris, France
[3] Univ. Montpellier, CNRS, UMR 5554, Institut des Sciences de l'Evolution de Montpellier (ISEM), 34095 Montpellier cedex 05, France
[4] Univ. Bordeaux, CNRS, UMR 5805 Environnements et Paléoenvironnements Océaniques et Continentaux (EPOC), F-33615 Pessac, France
[5] Geotop, Université du Québec à Montréal (UQAM), 201 Avenue du Président Kennedy, Montréal, Québec H3C 3P8, Canada

* Corresponding author : Vincent Coussin, email address : vincent.coussin@univ-brest.fr

Abstract :

The Mediterranean Sea is generally described as an oligotrophic area where primary productivity is limited to a few coastal environments with nutrient-enriched fluvial input. However, several studies have revealed that the hydrology of the western Mediterranean has major seasonal productive patterns linked either to significant riverine input or to seasonal upwelling cells. This study aims to: i) discuss organic microfossils (i.e. pollen and dinoflagellate cyst assemblages, as well as other non-pollen palynomorphs) from two different productive areas of the western Mediterranean Sea, and ii) examine the importance of the interconnections between marine and continental influences responsible for modern palynomorph distributions. Based on 25 samples from the Gulf of Lion (GoL) and Algerian Margin, this study key findings are: i) that GoL marine productivity is driven by the combination of discharge from the Rhone River and seasonal upwelling mechanisms, ii) that the strong pro-ductive pattern of the northern African coast is driven by water density front mixings and related upwelling. These two patterns are discussed in the light of major links that provide a better understanding of the signatures of marine and continental bio-indicators. Typical differences in vegetation across the north-south climate gradient in the western Mediterranean Basin are highlighted by the larger ratio of Euro-Siberian to Mediterra-nean pollen taxa in the northern sector. Synoptic maps also illustrate the complex interactions of environmental drivers determining the distributions of continental and marine palynomorphs in the western Mediterranean Sea.

Highlights

► Modern distribution of dinocyst taxa in the Western Mediterranean basin. ► Enlarging the Northern Hemisphere dinocyst database. ► Discussing new palynological assemblages accross hydrological and climatic gradients. ► Linking dinocyst oceanic signals to current continental vegetation. ► Exploring new continental bioindicators in marine sediments.

Keywords : Western Mediterranean Sea, Gulf of Lion, Algerian margin, Dinoflagellate cysts, Productivity, Fluvial discharge, Upwelling cells, Pollen and spores, Vegetation gradients, Non-pollen palynomorphs

1. Introduction

The Mediterranean Basin is made up of a series of semi-enclosed concentration basins stretching from the western Alboran Basin eastwards to the Levantine Basin. It is characterised by high evaporation and low freshwater input (i.e. precipitation and runoff), combining multiple climatic and hydrological influences, and is located between the mid-latitude storm path (i.e. westerlies) dominating northern and central Europe and the Azores High centred on North Africa (López-Moreno et al., 2011). High average surface salinity increases from the Strait of Gibraltar (< 37 psu) to the east (> 37.5 psu) of the basin (La Violette, 1986). Under the decreasing influence of Atlantic water from west to east, the Mediterranean Sea shows a strong hydrological contrast between its western and eastern basins (Béthoux, 1979, 1984). In addition, the Mediterranean Sea region experiences a typical seasonal cycle marked by cold wet winters and warm dry summers. This region is therefore characterised by a strong seasonality (i.e. seasonal differences in temperature) with adapted ecosystems. Mediterranean vegetation is an excellent example of this, with exceptional diversity (25 000 to 30 000 species and subspecies) and numerous endemic species (Médail and Quézel, 1997).

Most of the Mediterranean Sea is oligotrophic, with low nitrate and phosphate concentrations representing important limiting factors for primary productivity (Berland et al., 1979; Lazzari et al., 2016). However, some parts of the western Mediterranean Basin (WMB) can be considered as productivity hotspots (Margalef, 1985), such as the Alboran Sea gyres (Garcia-Gorriz and Carr, 2001; Oguz et al., 2014; Yebra et al., 2018), the Adriatic Sea around the Pô River mouth (Zonneveld et al., 2009), or coastal WMB areas characterised by enhanced nutrient-enriched fluvial discharge (Fig. 1b). On the northern side, the Rhône represents the largest river discharge to the WMB via a large freshwater plume extension responsible for terrigenous inputs to the Gulf of Lion (GoL) and supports half of the planktonic productivity of this area (Coste, 1974; Morel et al., 1990). On the southern side of the WMB, a frontal coastal zone along the Algerian Margin (AM) extends to 3°E. This haline front between Atlantic and Mediterranean surface waters (Lohrenz et al., 1988a; Arnone et al., 1990; Perkins and Pistek, 1990) accounts for strong vertical mixing and high nutrient and phytoplankton biomass concentrations (e.g. Sournia, 1973; Lohrenz et al., 1988a; Raimbault et al., 1993; Taupier-Letage et al., 2003). In addition, flash floods in autumn-winter, recognised as major erosive factors on land, represent an additional input of terrigenous sediments and, thus, of organic and inorganic particles and nutrients to the AM (Guizien et al., 2007; Tzoraki and Nikolaidis, 2007; Lombo Tombo et al., 2015).

Present-day environmental conditions, therefore, seem to make the WMB a suitable region to investigate modern Mediterranean dinocyst assemblages. Previous studies have shown that the distribution of dinocyst assemblages follows latitudinal and nearshore-offshore gradients, with maximum diversity along the continental margins, especially in warm areas, with productive conditions commonly supporting heterotrophic dinocyst taxa development (e.g. Marret and Zonneveld, 2003; de Vernal et al., 2020; Marret et al., 2020). The diversity of dinocyst assemblages is highlighted in the updated and standardized Northern Hemisphere 'modern' dinocyst database (71 taxa, n = 1968 surface sediments, 17 environmental parameters; de Vernal et al., 2020), which includes the WMB (n = 79 sites) but no surface sediment from the GoL or AM, despite their singular hydrological conditions and trophic regimes. The present study thus focuses, for the first time, on modern palynological data (pollen, dinoflagellate cysts or 'dinocysts', and other non-pollen palynomorphs or 'NPPs') from surface sediments distributed in the GoL (six samples) and AM (nineteen samples). Furthermore, terrestrial bio-indicators (pollen grains and continental or freshwater NPPs) also provide new information regarding palynomorph distribution in marine sediments in northern and southern WMB watersheds, hydro-climatic factors, and taphonomic sediment dispersal processes responsible for their dispersion and detection in the marine realm. These results will serve as a reference for further Holocene palynological investigations in both GoL and AM areas (Coussin, 2021).

2. Environmental context of the western Mediterranean Basin

2.1. Atmospheric pattern characteristics

The WMB is characterised by a local-scale climate due to a complex topography modifying large-scale atmospheric currents (Lionello et al., 2006). The GoL has an average temperature of 24°C in summer and around 8°C in winter, and highly irregular low rainfall (mean 650 mm/yr, range 15 to 100 mm/month). The AM is characterized by an average temperature of 26°C in summer and around 14°C in winter. It also has highly irregular rainfall (mean 550 mm/yr, range 3 to 110 mm/month).

During the autumn-winter, the WMB climate is generally influenced by the mid-latitude North Atlantic atmospheric circulation, especially the westerlies, as well as by continental polar air masses, channelled via the orographic networks bordering the northern Mediterranean margin (e.g. Mistral towards the GoL via the Rhône valley; Jiang et al., 2003; Fig. 1a), which also leads

to strong evaporation and cooling of surface waters. The North Atlantic Oscillation (NAO; Hurrell, 1995; Hurrell et al., 2003) is the natural mode of atmospheric variability that explains most of the variation in the WMB weather regimes at seasonal and inter-annual timescales. The NAO has direct impacts on the direction and intensity of the westerlies blowing over the WMB and, therefore, on mean seasonal precipitation regimes and related fluvial discharge. On the one hand, most pronounced winter cold events generally correspond to positive phases of the NAO (Moses et al, 1987; Maheras et al., 1999). On the other hand, negative phases of the NAO, corresponding to periods of weakening and southward displacement of the Azores High, are associated with wet winters (e.g. Maheras et al., 1999; Lolis et al., 2002; Dünkeloh and Jacobeit, 2003; López-Moreno et al., 2011). Additionally, during negative modes of the East Atlantic (EA) pattern, the second prominent mode of low-frequency variability over the North Atlantic for all months, the stagnation of a high-pressure cell over the north-western Atlantic Basin drives north-easterly cold air currents across Europe, especially through the Rhône River valley (Najac et al. 2009), which then cause the most intense Mistral winds to occur over the WMB (Skliris et al., 2012; Papadopoulos et al., 2015).

During the spring-summer, the so-called Sirocco wind events occur due to the eastward displacement of depression cells in the southern Mediterranean Basin (Lionello et al., 2006). This results in hot and dry southerly air masses over the WMB, with intermittent intense dust-laden winds from the Saharan desert (Prospero, 1996, Lionello et al., 2006). These wind events cause severe droughts, especially in the southern Mediterranean Basin, and particularly along the AM. The GoL, located in the north-western part of the WMB, is subject to the dual influence of northerly Atlantic and southerly African winds, as well as to interactions between mid-latitude westerlies and topographic effects of the Alps and Pyrenees. These geographic and topographic effects are responsible for several climatic gradients, including an increasing precipitation gradient from the south to the north of the WMB (Lionello et al., 2006). Moreover, the Algerian coast shows an increasing precipitation gradient from west to east due to the Mediterranean storm track trajectory focusing precipitation on the eastern zones (Lionello et al., 2006).

2.2. Hydrographic and hydrological patterns

The Mediterranean Sea is characterized by an overall excess of evaporation resulting in a deficient water balance (Béthoux, 1979, 1984; Bryden and Kinder, 1991; Béthoux and Gentili, 1994; Gilman and Garrett, 1994; Tsimplis et al., 2006; Skliris et al., 2018). Consequently, mean

salinity increases from the Strait of Gibraltar (< 37 psu) to the east of the Mediterranean Basin (> 37.5 psu) under the decreasing influence of the Atlantic surface waters layer from west to east (La Violette, 1986; Béthoux, 1999).

More precisely, at the Strait of Gibraltar, Atlantic surface water layers known as the Modified Atlantic Waters (MAW) enter the WMB in the Alboran Sea. Then, the strong Coriolis-driven MAW flux along the Spanish coast initiates the formation of two anticyclonic gyres (the Western Alboran Gyre or 'WAG' and the Eastern Alboran Gyre or 'EAG'; Fig. 1a). The degree of development of the EAG controls the position and intensity of the Almeria-Oran front (Tintoré et al., 1988; Rohling et al., 1995, 2009; Viúdez and Tintoré, 1995), 35 km wide and 200 m deep. This front marks the deflection of the MAW towards Oran along the AM, then forming the Algerian Current (AC; Fig. 1a; Millot, 1987; Millot, 1999, Millot and Taupier-Letage, 2005), which finally splits into two branches across the Sicilian Strait (Fig. 1a). The first of these leaves the WMB towards the eastern Mediterranean Basin while the second flows northward in the WMB and becomes the Northern Current (NC; Fig 1a).

a. The Algerian Margin

Along the AM, the AC (Fig. 1b) undulates eastward at 30–40 km from the coast to 3°E (Millot, 1985, 1987; Arnone and La Violette, 1986; Arnone et al., 1990; Perkins and Pistek, 1990). The Coriolis effect, coupled with the irregularity of the North African coast, also generates wind-driven eddies up to 3°E (Millot, 1999). These current instabilities are also responsible for northward coastal current influences and, therefore, the extension of low salinity surface waters offshore (Millot, 1999; Millot and Taupier-Letage, 2005). The WMB is generally oligotrophic (Fig. 1b), but deep Mediterranean waters, especially Levantine Intermediate Waters, are enriched in dissolved nutrients while surface layers are poorly enriched in nitrates. However, the meeting of Atlantic and Mediterranean waters in the Alboran Sea (forming the MAW followed by the AC; Fig. 1a) forms a marked haline density front that persists up to 3°E (Lohrenz et al., 1988a; Arnone et al., 1990; Perkins and Pistek, 1990). This haline density frontal zone is linked to strong vertical mixing (up to 100 m depth, Raimbault et al., 1993) and is described as a major production area where nutrient and phytoplanktonic biomass concentrations are high compared with the WMB (Sournia, 1973; Lohrenz et al., 1988a; Raimbault et al., 1993; Fig. 1b). Close to the coast, isopycnal mixing brings nutrient-enriched waters from the nutricline (150 m deep; Raimbault et al., 1993; Moutin and Raimbault, 2002) to the photic zone while, offshore, diapycnal mixing (i.e. crossing the haline front) brings deeper nutrients to the surface (Raimbault et al., 1993). Westward, from 0° to 2°E, offshore wind,

probably caused by low barometric pressure cells under strong solar heating, induces seasonal coastal upwelling (Bakun and Agostini, 2001).

In addition, on the AM, fluvial discharge are generally weak from April to September. Flash floods from *oueds* (i.e. wadis or arroyos) then occur in autumn–winter. Despite their occasional nature, these fluvial discharge are major erosive factors in the AM watersheds, carrying terrigenous detritus, including organic and inorganic particles and nutrients (Guizien et al., 2007; Tzoraki and Nikolaidis, 2007).

b. The Gulf of Lion

In the GoL, the NC (Fig. 1a) partly penetrates the inner shelf, following the coast and forming a secondary current when the Mistral intensity is weak (Millot, 1987; Millot, 1990; Millot, 1999; Millot and Taupier-Letage, 2005). The hydrological configuration is a combination of the Rhône River deflection under the Coriolis force and of the NC (Millot, 1990; Bakun and Agostini, 2001). Under the Mistral and Tramontane cold continental wind influences, intense surface water cooling is seasonally recorded during the autumn-winter and there is a southward deflection of the Rhône River discharge to the open sea. Also, Mistral and Tramontane winds generate summer-autumn coastal upwelling cells along the shore (between the French cities of Montpellier and Marseille), including the Rhône River delta area (Millot, 1979; Millot and Wald, 1981, Johns et al., 1992; Estournel et al., 2003; Campbell et al., 2013). Conversely, downwelling occurs periodically, especially during winter, leading the cold-dense waters to sink following the canyons that cut the continental shelf (Millot, 1987; Millot, 1990; Millot, 1999; Bakun and Agostini, 2001; Millot and Taupier-Letage, 2005). From spring to summer, a strong stratification develops that separates GoL surface water layers (0 to 20 m deep; 20°C) from subsurface waters (> 20 m; 13.5°C).

With a flow rate of 1690 $m^3 s^{-1}$ (Moutin et al., 1998), the Rhône River is the largest freshwater input to the WMB. Under the effect of the Coriolis effect, the Rhône freshwater plume extends westwards over several tens to hundreds of kilometres under the influence of the wind and propagates over a thickness of one to several metres. In the GoL, fine particulate and dissolved organic and inorganic terrigenous inputs from the Rhône River provide nutrients for about 50% of the planktonic productivity (Coste, 1974; Morel et al., 1990).

2.3. Present-day vegetation cover on western Mediterranean watersheds

In general, the terrestrial plant cover of western Mediterranean areas can be divided into vegetation belts defined by temperature and precipitation, altitude, slope orientation and soil type (e.g. Ozenda, 1975; Rivas Martinez, 1982; Polunin and Walter, 1985; Barbero et al., 1981; Benabid, 1982; Quezel and Medail, 2003).

In Algeria, the thermo-Mediterranean vegetation belt is composed of *Olea*, *Pistacia,* sclerophyllous shrublands and xerophytic taxa, with steppe or semi-desert taxa, such as *Artemisia,* Amaranthaceae and *Ephedra*. This vegetation belt is found in lowlands and near coastal areas up to 1000 m and constitutes the main vegetation westward of the AM. At higher altitudes, the meso-Mediterranean belt is composed of sclerophyllous oak forest and associated with humid-temperate oak forest (dominated by deciduous *Quercus* and Ericaceae in association with *Juniperus* and *Cupressus*). This belt extends to 1400–1500 m. The supra-Mediterranean belt characterizes the higher altitudes from 1400 to 2300 m, comprising a specific coniferous forest of North African species of *Pinus, Abies* and *Cedrus*. Above this, the oro-Mediterranean vegetation belt extends to 2800 m in the high Atlas, with *Juniperus* strongly represented (i.e. open forest taxa or arborescent *mattorals* or shrublands). Finally, the alti-Mediterranean belt corresponds to the European mountainous grassland belt and represents the highest vegetation in the mountainous regions. This belt is composed of scattered Chamaephytae taxa, such as *Erica, Rosmarinus* and other Lamiaceae, *Ilex* or *Artemisia*.

In the GoL, coastal vegetation extends from the shoreline to the inner zones up to 100–200 m. Cyperaceae (e.g. *Carex*) or Ranunculaceae represent the hydrophilous vegetation dominating the Rhône River delta area. Amaranthaceae and Caryophyllaceae represent the well-developed halophitic coastal vegetation of the western GoL coast. The thermo-Mediterranean belt is mainly represented by *Olea, Cistus*, *Pistacia,* sclerophyllous shrublands and, to a lesser extent than in Algeria, xerophilous taxa (e.g. *Artemisia,* Amaranthaceae or *Ephedra*). This vegetation belt extends from the coast to 400 m. Sclerophyllous oak forest of *Quercus ilex* and *Quercus suber* is characteristic of the meso-Mediterranean belt, in association with the humid-temperate oak forest taxa (e.g. deciduous *Quercus*, *Fagus*, *Betula, Carpinus*, Ericaceae). This belt extends from 400 to 900 m and corresponds to the European temperate foothills. From 900 to 1300 m, the supra-Mediterranean belt is composed of temperate deciduous forest (e.g. deciduous *Quercus*, *Fagus*) associated with some mountainous conifers (e.g. *Abies*, *Pinus*, *Cedrus*). In the GoL sediments, observations of *Picea* and *Abies* (trees only growing in the Alps) pollen imply

a north-eastern source of continental palynomorphs. The oro-Mediterranean belt from 2200 to 2500 m corresponds to the sub-alpine European belt with the discontinuous representation of *Juniperus*. The alti-Mediterranean belt, above the arboreal altitudinal limit, corresponds to the European alpine belt and is characterized by sparse shrublands.

3. Material and methods

3.1. Core tops

a. Geographical and cruise details of the study samples

Surface sediments were collected from 25 sites (6 in the GoL and 19 in the AM, from 0° to 8°E; Fig. 1c) during the cruises GMO1 (2001), GMO2-CARNAC (2002), MARADJA (2003), BEACHMED (2004), MARADJA2 (2005), PRISME (2007) and RHOSOS (2008). Samples, consisting of 1 to 3 cm^3 from the upper half centimetre of each gravity core, were selected for different bathymetries in order to compare palynomorph distribution in the two different study areas GoL and AM (Table 1).

b. Radionuclide dating

To confirm the modern ages of the top cores, activities of ^{210}Pb, ^{226}Ra and ^{137}Cs radioactive isotopes were measured on each sediment sample using a low-background, high efficiency well-shaped germanium detector at the EPOC laboratory (CNRS, University of Bordeaux).

On the one hand, ^{210}Pb presents excesses ($^{210}Pb_{xs}$) that decrease with depth in sediments according to its half-life (22.3 years). $^{210}Pb_{xs}$ is determined as the difference of the measured total ^{210}Pb and ^{226}Ra, its parent isotope in the sediment (Schmidt et al., 2005). The highest $^{210}Pb_{xs}$ activities are observed at the top of sediment cores and decrease exponentially with depth to reach a low to negligible level for sediments older than 100 years. On the other hand, ^{137}Cs is an artificial radionuclide, first detected in marine sediments in the middle of the 20th century, characterized by well-known pulse inputs (e.g. nuclear weapon test fallout in the sixties).

The uppermost layer (0–1 cm) of each core was measured by gamma spectrometry to determine the activities of $^{210}Pb_{xs}$ and ^{137}Cs, which were interpreted according to the following rules: core tops presenting high activities of both radionuclides are considered recent (< 30 years); core tops with moderate $^{210}Pb_{xs}$ are classified < 60 years or < 100 years, depending on the level of ^{137}Cs; core tops in which there are no detectable activities of $^{210}Pb_{xs}$ and ^{137}Cs are considered older than 100 years (Table 1).

3.2. Palynological analyses

a. Palynological treatments and palynomorph identification

The 25 samples (Fig. 1c) were processed with the same palynological protocol for palynomorph extraction, allowing direct comparison between terrestrial (pollen, spores, freshwater microalgae and other continental NPPs) and marine (dinocysts, other marine microalgae and foraminiferal linings) palynomorphs on the same palynological slides. The preparation technique (Geo-Ocean laboratory, IUEM, University of Brest), conducted on the <150 µm fraction, followed the standardized palynological protocol of de Vernal et al. (1999), slightly adapted at the EPOC laboratory (University of Bordeaux, http://www.epoc.u-bordeaux.fr/index.php?lang=fr&page=eq_paleo_pollens). It includes chemical treatments (cold HCl: 10, 25 and 50%; cold HF: 45 and 70%, to remove carbonates and silicates, respectively) and sieving through single-use 10-µm nylon mesh screens. In order to avoid any selective dinocyst degradation during sample treatments, no oxidative agents nore heavy liquid techniques were used.

For each sample analysed, a minimum of 100 dinocysts and 150 pollen grains were identified (except the overrepresented taxa *Pinus*; Turon, 1984; Heusser and Balsam, 1985) following the systematics of Fensome et al. (1993) and identifications based on Reille (1992), respectively, using a Zeiss microscope (Axioscope A1) at 630x magnification. The threshold of 100 individuals is required to identify 99% of major (>5%) species (Fatela and Taborda, 2002). It should be noted that, for dinocysts only, the AM samples PSM-KS33, PSM-KS34 and PSM-KS35 were grouped and labelled 'site PSM-KS33-34-35', due to the difficulty of reaching the statistically robust threshold of 100 dinocysts in these three individual samples. *Brigantedinium* spp. includes all round brown dinocysts without processes. *Echinidinium* spp. includes all brown dinocysts with typical *Echinidinium* spine-like processes not determined to species level. *Spiniferites* spp. includes all *Spiniferites* dinocysts not determined to species level.

Autotrophic dinocysts (i.e. those from dinoflagellates with a phototrophic or mixotrophic nutrition strategy) include species with chlorophyll pigments, while heterotrophic dinocysts (i.e. from dinoflagellates with a strict heterotrophic strategy of nutrition) are indirectly related to abundant food resources, especially diatoms, as commonly shown in upwelling areas (Wall et al., 1977; Lewis et al., 1990; Marret, 1994; Biebow, 1996; Zonneveld et al., 1997a, 2001; Targarona et al., 1999; Bouimetarhan et al., 2009; Penaud et al., 2016). Consequently, a ratio of heterotrophics to autotrophics (H/A) is commonly adopted in ecological and paleoecological

studies and takes into account 'strict' heterotrophic counts vs. the other taxa identified in dinocyst assemblages, making it possible to indirectly discuss productivity conditions in surface waters. The 'Fungal spores undetermined' group includes all the fungal spores that cannot be determined to the genus or species level or to a type code relative to the description available in the literature.

Relative abundances (%) were calculated for pollen and dinocyst assemblages. Pollen percentages were calculated using the pollen main sum without *Pinus*. *Pinus* relative abundance calculations were based on the total pollen sum. Continental NPP relative abundances were calculated based on a total sum including the pollen main sum without *Pinus* and the sum of spores and other continental NPPs (van Geel et al., 1972; Cugny et al., 2010; Miola, 2012). Palynomorph concentrations (number of specimens/cm^3 of dry sediments) were calculated using the marker grain method (Stockmarr, 1971; de Vernal et al., 1999; Mertens et al., 2009) by adding aliquot volumes of *Lycopodium* spores before the palynological treatment of each sample, with these exotic spores being counted in parallel with the studied marine and continental palynomorphs.

b. Statistical analysis on palynological results

Palynological spectra for pollen and dinocyst assemblages were constructed with the Tilia software (Grimm, 1990), which also allows the definition of the most parsimonious number of zones between sampling sites according to the CONISS model (Grimm, 1987).

Palynological taxonomic indexes (dominance, species richness, Margalex index) were quantified by statistical analyses using the PAST program, version 4.06b (Hammer et al., 2001; indexes explained in Hammer and Harper, 2008). In addition, multivariate analyses were performed with the PAST program: detrended correspondence analysis (DCA) for dinocyst data and canonical correspondence analysis (CCA) for dinocyst and pollen data. DCA was applied to dinocyst assemblages (expressed in percentages) in the framework of the enlarged n = 102 WMB dinocyst database (Fig. 1c) to map dissimilar samples between the 79 WMB sites from de Vernal et al. (2020) vs. the 6 new sites sampled in the GoL and the 17 new sites sampled in the AM (including the 3 sites amalgamated into one). CCA was also performed with both dinocyst percentage data and environmental data to identify the main factors that explain marine palynomorph distribution. In addition, CCA was applied to dinocyst and continental palynomorphs (expressed in concentrations) considering only the n = 17 sites of the AM.

For the CCA analyses, we extracted the environmental parameters corresponding to the new studied sites (Fig. 1c) according to the same procedure as used in de Vernal et al. (2020). Sea-

surface temperature (summer and winter SSTs), sea-surface salinity (summer and winter SSSs), dissolved oxygen (DO), as well as nutrient (phosphate-P, nitrate-N) and silicate (Si) concentrations were extracted from the World Ocean Atlas (WOA) 2018. Annual primary productivity (PP) data were calculated using the vertical generalized production model (VGPM) algorithm applied to the 2002–2017 chlorophyll data provided by the NASA's Moderate Resolution Imaging Spectroradiometer (MODIS) program (https://modis.gsfc.nasa.gov/data/dataprod). The distance to the coast (Dcoast), expressed in km, was calculated with ARCGIS using geodetic distances between features. This method is based on the World Geodetic System (WGS 84; https://gisgeography.com/wgs84-world-geodetic-system/), which takes into consideration the curvature of the spheroid and deals with data near the dateline and poles. Bathymetric data (for the variable Depth) were extracted from the General Bathymetric Chart of the Oceans (GEBCO 2014, version 20141103, http://www.gebco.net).

4. Results

Dinocyst results led us to class the sites into four groups based on the total sums of square values, which is higher than the three groups indicated using the CONISS cluster analysis (Fig. 2a). These four zones correspond to distinct hydrological conditions in the GoL and AM (Fig. 2a). Since samples PSM-KS33, PSM-KS34 and PSM-KS35 were grouped together (labelled as site PSM-KS33-34-35) due to low dinocyst counts, results presented hereafter represent n = 23 points (6 in the GoL and 17 in the AM) for dinocyst assemblages and n = 25 points (6 in the GoL and 19 in the AM) for pollen assemblages. Known ecological affinities were further used to define dinocyst ecological associations (Marret and Zonneveld, 2003; Zonneveld et al., 2013), as shown above the dinocyst spectra on Fig. 2a. Similarly, the knowledge of modern vegetation allowed us to define the pollen source vegetation types, including anthropogenic environments (Ozenda, 1975; Rivas Martinez, 1982; Polunin and Walter, 1985; Barbero et al., 1981; Benabib, 1982, 2000; Quezel and Medail, 2003), as shown above the pollen spectra on Fig. 2b.

4.1. Dinoflagellate cysts

a. Diversity and concentrations

Total dinocyst diversity reached a total of 36 different taxa for the new samples from the GoL and AM sites with a mean value of 19 taxa/sample (Fig. 2a). This average is close to the one

(17 taxa/sample) found in the modern dinocyst database of de Vernal et al. (2020) for the WMB (n = 79 sites).

Major dinocyst taxa, including all those exceeding the 1% threshold at least once among all the studied assemblages, are shown in Fig. 2a. We grouped dinocyst taxa (Fig. 2a) according to their ecological affinities (Marret and Zonneveld, 2003; Zonneveld et al., 2013; Penaud et al., 2020; van Nieuwenhove et al., 2020; Marret et al., 2020): i) the 'cool water-full oceanic' group (e.g. *Nematosphaeropsis labyrinthus* and *Bitectatodinium tepkiense*), ii) the 'thermophilous-full oceanic' group (*Impagidinium* species dominated by *Impagidinium aculeatum* and *Impagidinium patulum*), iii) the 'outer neritic' group (e.g. *Spiniferites mirabilis* and *Operculodinium centrocarpum*), iv) the 'inner neritic' group (e.g. *Spiniferites ramosus, Spiniferites bentorii, Spiniferites belerius, Spiniferites membranaceus*), and v) the 'estuarine-fluviatile' group (e.g. *Lingulodinum machaerophorum* and coastal heterotrophic taxa such as *Echinidinium* spp.). Heterotrophic taxa from the 'estuarine-fluviatile' group also relate to the 'coastal productivity' group including *Echinidinium* species and the Miscellaneous Peridinioid Cysts (MPCs, e.g. *Selenopemphix nephroides*, *Selenopemphix quanta*, *Lejeunecysta* spp., *Trinovantedinium applanatum*). Finally, the 'upwelling' group is mainly represented by *Brigantedinium* spp., also associated with MPCs.

The 'a' cluster (1 site), formed of sample KGMO-10 only (Fig. 2a, from the base of the GoL continental slope), is dominated by *O. centrocarpum* (22%) associated with *N. labyrinthus* (15%). Dinocyst concentration is 1232 cysts/cm^3. According to the dinocyst assemblage, this cluster represents full-oceanic oligotrophic conditions.

The 'b' cluster (4 sites) is dominated by *L. machaerophorum* (15 to 45%), *Brigantedinium* spp. (mean 12%), *S. belerius* (mean 6%), *S. nephroides* (mean 6%) and *T. applanatum* (mean 6%) and is characterized by the highest diversity of heterotrophic taxa. Average dinocyst concentration is 985 cysts/cm^3. This cluster corresponds to fluvial-influenced coastal assemblages.

The 'c' cluster (3 sites) is dominated by *S. mirabilis* (20 to 60%), *O. centrocarpum* (mean 15%) and *I. aculeatum* (mean 15%). It is characterized by the lowest values of heterotrophic taxa (mean 7%). The average dinocyst concentration is 1182 cysts/cm^3. This group corresponds to full-oceanic and oligotrophic conditions.

The 'd' cluster (15 sites) is largely dominated by *Brigantedinium* spp. (20 to 40%) and *S. mirabilis* (10 to 40%). The major species are *O. centrocarpum* (mean 11%), *L. machaerophorum* (mean 6%), *S. ramosus* (mean 5%) and *I. aculeatum* (mean 4%). This group is characterized by the maximum numbers of heterotrophic taxa, especially *Brigantedinium* spp.

(mean 42%). The average dinocyst concentration is 1102 cysts/cm^3. This cluster typically represents full-oceanic conditions characterized by seasonal upwelling productivity.

b. Distribution of major dinocyst taxa

Selected dinocyst results have been plotted on maps to demonstrate inshore-offshore distributions and GoL and AM specificities (Fig. 3a). Dinocyst diversity is higher offshore for both studied areas. On the AM, dinocyst concentrations are generally higher (mean 1106 and maximum 2427 cysts/cm^3) than in the GoL (mean 1134; maximum 1666 cysts/cm^3), while decreasing from west to east on the AM. Upwelling zones are marked by *Brigantedinium* spp. in the coastal zone of the GoL and the distal zone of the western AM between 2 and 6°E. *Spiniferites mirabilis* is poorly represented in the GoL, with only one occurrence higher than 10% (sample KIGC-01) in the seaward margin of the study area, while this outer neritic taxon is strongly represented along the much narrower North African coast where most sites are located in the outer shelf continental slope area. *Lingulodinium machaerophorum* shows maximum abundances in the near-coastal sites of the GoL while its abundances are three times lower on the AM including the coastal sites. Finally, the full-oceanic *Impagidinium* species mainly occur in the seaward sites of both GoL and AM, with a slight increase from west to east on the AM.

4.2. Pollen assemblages

a. Diversity and concentration

Major pollen taxa (exceeding a threshold of 1% at least once among the total studied assemblages) and some minor taxa associated with human-related impacts, as well as continental NPPs such as trilete spores (bryophytes and pteridophytes), freshwater algae (*Concentricystes*-type and *Pediastrum*-type) and fungal spores (including all Ascomycota and Basidiomycota spores; van Geel and Aptroot, 2006; Cugny et al., 2010), are shown in Fig. 2b. Among the fungal spores, we also distinguished *Glomus* (HdV-207; van Geel et al., 1989) and coprophilous taxa (type spores of *Sporormiella*: HdV-113, van Geel et al., 2003; *Sordaria*: HdV-55, van Geel, 1978; *Delitschia*: TM-023A/B, Cugny et al., 2010; *Coniochaeta*: HdV-172, van Geel et al., 1983). Pollen diversity reaches a total of 70 different taxa for all the 25 studied samples and a mean value of 37 different taxa per sample (Fig. 2b).

The ‘a’ cluster (1 site) is dominated by arboreal taxa (AP), reaching 60%, with a major representation of Cupressaceae (25%, consisting of *Cupressus* and *Juniperus*), mountainous

forest taxa (5%; e.g. *Abies*), and Eurosiberian forest taxa (12%; e.g. deciduous *Quercus*), accompanied by semi-arid indicators (12%; e.g. *Artemisia*), as well as coastal (9%; e.g. Amaranthaceae) and other herbaceous (11%; e.g. Poaceae) taxa. This cluster is characterized by the highest values of freshwater algae (2%). Pollen concentration (without *Pinus*) is 1017 grains/cm^3.

The 'b' cluster (4 sites) shows the highest values of AP percentages (mean 57%), mainly represented by *Quercus ilex* (mean 9%) and deciduous *Quercus* (mean 12%). The cluster is also associated with Cupressaceae (mean 14%), mountainous forest taxa (mean 6%; i.e. *Abies, Picea* and *Cedrus*), semi-arid (mean 7%; e.g. Amaranthaceae) and open or clear ground indicators, including Poaceae (mean 33%). Anthropic taxa such as *Cerealia* and *Plantago lanceolata* represent about 2% of the total pollen assemblages. Mean pollen concentration (without *Pinus*) is 2482 grains/cm^3 and maximal values reach 6483 grains/cm^3.

The 'c' cluster (3 sites) is characterized by about 50% tree pollen, which is mainly represented by Mediterranean forest taxa (mean 10%; e.g. *Quercus ilex*), in addition to semi-desert pollen from arid or coastal (mean 11%; e.g. Amaranthaceae) and open or clear ground (mean 37%; e.g. Cichorioideae and Poaceae) vegetation including anthropogenic taxa (0.6%; e.g. Cerealia, *P. lanceolata*, *Rumex*). Mean pollen concentration (without *Pinus*) is 2385 grains/cm^3 and maximal values reach 2946 grains/cm^3.

The 'd' cluster (15 sites) is characterized by the lowest tree pollen percentages (mean 36%), marked by *Quercus ilex* (mean 7%), associated with *Juniperus* (mean 4%) and *Olea* (mean 5%). In this cluster, deciduous *Quercus* (mean 4%) is the only Eurosiberian AP component and *Cedrus* (mean 0.5%) sign for the mountainous forest. In this cluster, the open ground vegetation taxa including Cichorioideae (mean 23%) and Poaceae (mean 8%), show their highest percentages (mean 46%). Accompanying pollen indicators are semi-arid vegetation taxa (mean 15%), including Amaranthaceae (mean 9%) and *Artemisia* (mean 2%). Anthropogenic taxa percentages are low (about 0.9%). This cluster is also characterized by the highest representation of undifferentiated (mean 5%) and coprophilous (mean 1%) fungal spores, *Glomus* type (mean 8%), and the lowest representation of freshwater algae (mean 0.1%). Mean pollen concentration (without *Pinus*) is 6831 grains/cm^3 and maximal values reach 17 748 grains/cm^3.

b. Distribution of major pollen taxa

Selected pollen results are plotted on maps to highlight continental palynomorph distributions as well as GoL and AM specificities (Fig. 3b). Equivalent mean species richness (about 38

different taxa) is observed on both AM and GoL study areas. GoL sites show lower mean pollen concentrations (with *Pinus*: 2953 grains/cm^3; without *Pinus*: 1460 grains/cm^3) than the AM sites (with *Pinus*: 7207 grains/cm^3; without *Pinus*: 5535 grains/cm^3). A higher representation of AP is noted in the GoL (mean 58%) compared with the AM (mean 37%), and conversely for the open or cleared ground vegetation. *Pinus* percentages are higher in the GoL (mean 51%) compared with the AM (mean 19%). *Pinus* percentages increase with the distance to the coast. In addition, the Eurosiberian forest taxa (mainly figured out by deciduous *Quercus*) are more highly represented in the GoL (mean 10%) compared with the AM (mean 5%). Conversely, the Mediterranean tree taxa (mainly *Quercus ilex*) are better represented in the AM area (mean 14%) than in the GoL (mean 8%). Altitudinal pollen taxa (*Abies*, *Picea* and *Cedrus*) are better represented in the GoL (mean 5%; slightly higher around the Rhône River mouth) than in the AM (mean 2%; slightly higher between 3°E and 4°E). Finally, the AM is characterised by higher concentrations of *Glomus* spores (mean 537 spores/cm^3) than the GoL (mean 158 spores/cm^3; with higher values near the Rhône River mouth).

5. Discussion

5.1. Statistical analysis on the new western Mediterranean Basin dinocyst database

a. Dinocyst taxa in relation to environmental parameters in the n = 102 WMB database

DCA analyses were performed on the enlarged WMB dinocyst database containing n = 102 samples, which includes the n = 79 samples from de Vernal et al. (2020) and the n = 23 new studied dinocyst assemblages (6 in the GoL and 17 in the AM; see Figs. 1c and 4a). Results clearly highlight the unique characteristics of the GoL and AM sites. The most distal GoL and AM sites (KMDJ-38, PSM-KS30, KIGC-01 and KGMO 10; Figs. 1c and 4a), characterised by full-oceanic dinocyst taxa, record assemblages like those already reported in the n = 79 database. Most of the new GoL and AM sites are characterised by high heterotrophic taxa percentages (means of 29 and 31%, respectively) compared to the initial database (mean 1%). These sites also correspond to the highest surface productivity values in the generally oligotrophic WMB (Fig. 1b). The new data suggest a gradient between ‘offshore’ assemblages, corresponding to oligotrophic conditions, and ‘inshore’ assemblage corresponding to

productive areas (Fig 4a). The newly added sites thus provide palynological information on environmental conditions that were not previously represented.

A CCA statistical analysis was also made on the enlarged WMB dinocyst database, including 21 taxa cross-referenced with 11 environmental parameters (Fig. 4b). The two axes of the CCA plot together explain 71% of the total variance (52% and 19% for axes 1 and 2, respectively. Axis 1 (horizontal orientation) shows a strong correlation with nitrate (N) and phosphate (P) concentrations and annual primary productivity (PP), suggesting dominant productive conditions on the left side of the plot (Fig. 4b). All the heterotrophic taxa (e.g. *Brigantedinium* spp., *T. applanatum*, *Lejeunecysta* spp., *Echinidinium* spp., *S. nephroides*, grouped *Selenopemphix quanta* and *Protoperidinium nudum*) are found in the 'productive' axis direction. Indeed, *Brigantedinium* spp. are typically reported for upwelling areas, with the associated taxa *Lejeunecysta* spp. and *T. applanatum* (e.g. Margalef, 1985; Marret and Zonneveld, 2003; Zonneveld et al., 2013). Conversely, the right side of axis 1 in Fig. 4b corresponds to oligotrophic conditions also associated with increasing seasonal SSS, summer SST, silicate and dissolved oxygen values. The *Impagidinium* species identified at the studied sites (especially *I. aculeatum* and also *I. patulum* to a lesser extent) are taxa representative of full-oceanic conditions here logically found in the 'oligotrophic' axis direction.

In addition, axis 2 (vertical orientation) of the CCA reveals inshore-offshore influence, as shown by increasing parameters such as 'Depth' and 'Distance to the coast' towards the top side of the plot (Fig. 4b). Both parameters are inversely correlated with higher *L. machaerophorum* abundances. Indeed, this latter taxon is a typical estuarine-sensitive taxon characterizing brackish environments and tolerating large drops in salinity close to river mouths and in relation to freshwater plume extensions (e.g. Pospelova et al., 2004; Wang et al., 2004; Giannakourou et al., 2005; Pospelova et al., 2005; Mertens et al., 2012; Ganne et al., 2016; Penaud et al., 2020). Interestingly, among heterotrophic taxa, MPC taxa such as *S. quanta* and *P. nudum* show a preference for coastal (i.e. inshore axis 2 direction; Fig. 4b) productive (left side of axis 1; Fig. 4b) conditions, and were referred to as 'coastal heterotrophics' in Penaud et al. (2020). Cysts of *Pentapharsodinium dalei* and *Echinidinium* spp. are known to occur in areas subjected to freshwater input and reduced salinity (Marret and Zonneveld, 2003; Zonneveld et al., 2013). In the CCA, both taxa are found in an intermediate position between coastal heterotrophic taxa and *Brigantedinium* spp., the latter tending to be more frequently recorded offshore (i.e. top of axis 2; Fig. 4b) in productive (left side of axis 1; Fig. 4b) conditions, i.e. where distal productivity is explained by increasing upwelling.

Finally, both seasonal SSS variables appear correlated with the summer SST variable and reflect the spring to summer seasonal stratification pattern observed in the WMB (described in section 2.2.b for the GoL). The strongest representation of *L. machaerophorum* in the GoL (Fig. 2a) in the WMB (Fig. 5g) corresponds to the Rhône River freshwater plume influence during autumn-winter. The coastal oligotrophic assemblage is characterized by *Spiniferites* (e.g. *S. mirabilis, S. pachydermus, S. ramosus, S. bulloides*) and by *Operculodinium* (e.g. *O. centrocarpum* and *O. israelianum*) species, occurring in well-oxygenated surface waters and warmer summer SST of temperate climate zones (e.g. Rochon et al., 1999; Esper and Zonneveld, 2007; Radi et al., 2007; Marret and Zonneveld, 2003; Pospelova et al., 2008; Zonneveld et al., 2013).

b. Dinocyst taxa in relation to environmental parameters in the n = 17 AM database

A CCA statistical analysis was also conducted on the AM studied sites (n = 17 sites), including 22 taxa (expressed in absolute concentrations) cross-referenced with 11 environmental parameters (Fig. 4c). The same approach was not taken as with the GoL samples because the 6 modern sites present in the database are not enough to undertake robust statistics. For the AM, both axes of the CCA plot explain 75% of the total variance (i.e. 54% and 21% for axis 1 and axis 2, respectively) and allow the main environmental gradients driving dinocyst distribution to be examined when considering only the AM.

Productive conditions in the AM study area are depicted by nutrient (P and N) concentration axes in the same direction as annual PP. These variables correlate with winter SST and Depth (Fig. 4c). The CCA sector corresponding to productive conditions includes two groups of taxa: i) *L. machaerophorum* and *Echinidinium* spp. (with also *S. ramosus, S. bulloides, S. quanta,* and cysts of *P. nudum, S. pachydermus, S. nephroides*), representative of the proximity to the coast, which may be a sign of occasional coastal river discharge on the AM, and ii). *Brigantedinium* spp. (with also *N. labyrinthus* and *Lejeunecysta* spp.), representative of a more distal signature that may reflect isopycnal and diapycnal-derived productivity conditions (Raimbault et al., 1993). Indeed, on the AM, seasonal coastal upwelling currently occur during spring to autumn under the influence of turning winds (Bakun and Agostini, 2001) superimposed on AC eddies (Millot, 1985; Arnone and La Violette, 1986; Millot et al., 1990). Cyclonic eddies of the AC occur offshore and generate surface layer nutrient enrichment and spring to autumn surface cooling via strong water and nutrient mixing (Morán et al., 2001). This is consistent with strong occurrences of *Brigantedinium* spp. in the AM. Upwelling mechanisms can also explain the correlation between *Brigantedinium* spp. and the cold-water taxon *N. labyrinthus*, and the anti-correlation with the summer SST axis (Fig. 4c). This

strengthens the idea of a major control of the intensity of the nutrient-rich water vertical fluxes on the magnitude of the AM productivity during spring to autumn (Raimbault et al., 1993). Keeping in mind the seasonal pattern of river discharge on the AM, far from that of the Rhône River in the GoL, the annual PP vs. Depth correlation (Fig. 4c) suggests two distinct mechanisms: i) a coastal productivity in proximal areas subjected to seasonal river runoff and discharge; and ii) an upwelling productivity offshore, with the frontal zone found between MAW and Surface Mediterranean Waters.

The winter SSS axis (Fig 4c) may be related to full-oceanic MAW influence in the WMB. This axis is correlated with higher concentrations of *S. mirabilis*, which we relate to low to moderate water column vertical mixing, contrary to the strong vertical mixing associated with *Brigantedinium* spp. Association of *S. mirabilis* with *T. applanatum*, the latter being an upwelling-sensitive taxon according to Zonneveld et al. (2013), indicate a MAW influence (Fig. 5e). The Atlantic influence is also supported by the occurrence of *S. septentrionalis, B. tepikiense* and *S. lazus*, which are North Atlantic taxa found in outer neritic-oceanic waters. In the AM, *O. israelianum* and *S. belerius* are located between the strong coastal river-discharge influence shown by *L. machaerophorum* and *Echinidium* spp. and the offshore MAW influence shown by *S. mirabilis* and *B. tepikiense*.

There are also strong correlations between the 'Distance to the coast' axis, and summer SST and SSS, suggesting that distal conditions are linked to the Surface Mediterranean Waters, and logically coincide with higher occurrences of the full-oceanic *Impagidinium* taxa. Finally, the CCA for the AM shows a correlation between the 'Distance to the coast' variable (as well as dissolved oxygen and silicate axes) and higher occurrences of *S. membranaceus* and *Achomosphaera* taxa.

c. Diversity and distribution of dinocyst taxa in the western Mediterranean Basin

Selected dinocyst results are mapped for the WMB in Fig 5, which considers the enlarged n = 102 dinocyst database and represents the newly studied sites with green circles.

First, as already pointed out in subsection 4.1.a., the two new studied areas (AM and GoL) have levels of species richness among the highest in the WMB, with a mean of 19 taxa/sample and a maximum of 24 taxa/sample in the GoL and AM sites, compared with the mean of 17 taxa/sample and maximum of 26 taxa/sample reported by de Vernal et al. (2020) (Fig. 5a).

Three maps of heterotrophic dinocyst percentages (Figs. 5b, 5c, 5d) indicate prevailing oligotrophic conditions in the WMB, except for the Alboran Sea, which is characterized by contrasted high productive conditions in the GoL and AM new sites. The upwelling-sensitive

taxa *Brigantedinium* spp. (Fig. 5c) occur in GoL areas characterised by Mistral wind-induced upwelling, and maximum *Brigantedinium* abundances are also found in the westernmost parts of the AM, along the AC isopycnal front extending to 3°E (see subsection 2.2.a.) and characterised by strong productivity, especially in the frontal external zones (Raimbault et al., 1993).

The outer shelf and slope parts of the GoL, under the influence of the cold Mistral continental wind, which itself induces downwelling in the mid-shelf area, have the highest occurrences of cold water-sensitive dinocyst taxa (Fig. 5e). Conversely, the temperate indicator *S. mirabilis* (Fig. 5f) shows strong occurrences in the southern part of the WMB from the Alboran Sea to the Sicilian Strait, and low representation in the northernmost part of the WMB. We suggest an unambiguous link between *S. mirabilis* and the MAW, and by extension with the AC flow. *Impagidinium* species mainly consist in *I. aculeatum* and *I. patulum* to a lesser extent, while *I. sphaericum, I. strialatum* and *I. velorum* show sparse and low occurrences in the WMB. Here, *Impagidinium* spp. distribution (Fig. 5g) characterizes full-oceanic areas of the WMB as well as the cosmopolitan North Atlantic taxon *O. centrocarpum* (Fig. 5h). The patterns of both these groups are consistent with the NC influence in the WMB. Interestingly, *Impagidinium* spp. distribution contrasts with that of *S. mirabilis*, considered as another halophilic taxon, here revealing the crucial role of north-to-south and east-to-west SSS and SST gradients in the WMB.

Distributions of coastal heterotrophs (*Echinidinium* spp., *S. quanta* and cysts of *P. nudum*; Fig. 5i) and of the freshwater-sensitive taxon *L. machaerophorum* (Fig. 5j) are related to nutrient-enriched river input and are mainly found in coastal environments subjected to seasonal fluvial discharge. This dinocyst association suggests that recurrent and strong terrigenous inputs sustain coastal productivity. It is also consistent with the modern estimation of terrigenous input (especially from the Rhône River) into the GoL, contributing up to half of the present-day productivity (Coste, 1974; Morel et al., 1990, Diaz et al., 2000; Galeron et al., 2014).

5.2. From land to sea: correlating land and marine information

a. Hydrological control of pollen assemblages along the Algerian Margin

In order to link continental and oceanic information provided by marine (Fig. 2a) and continental (Fig. 2b) palynomorphs in the AM (n = 17 sites; Fig. 6), a CCA was performed on the concentrations of main pollen (n = 11) and non-dinocyst NPP (n = 5) ecological groups (Fig. 6; groups on Fig. 2b). Inferred-environmental variables (Fig. 6) are represented by

concentrations of main dinocyst ecological groups (Figs. 4b and 4c: 'estuarine taxa' refers to *L. machaerophorum*, 'full-oceanic taxa' refers to *Impagidinium* spp., 'upwelling taxa' refers to *Brigantedinium* spp., and 'coastal productivity taxa' refers to grouped *Echinidinium* spp., *S. quanta* and cysts of *P. nudum*), as well as to geographical information on the studied sites (i.e. 'Distance from the coast' and 'Depth'). In the CCA, the two axes explain 83% of the total variance (53% and 30% for axis 1 and axis 2, respectively) and reveal the main environmental gradients driving the distribution of continental palynomorphs in the AM study area.

The ordination diagram shows that the increased bathymetry (see variable 'Depth' on Fig. 6) and outer neritic/offshore-oceanic location (see variable 'Distance to the coast' on Fig. 6) of the AM point in the same directions than the dinocyst variables 'upwelling' and 'coastal productivity' (Fig. 7). This may be due to the narrow width of the AM continental shelf and to the overrepresentation of offshore sites in this dataset (Fig. 1c). AM pollen and continental NPP groups vary along a geographical gradient according to the west-east vegetation pattern observed in Algeria (Fig. 3b). Dinocysts indicate gradually decreasing productivity from the western to the eastern AM (Fig. 3a), which is consistent with the vegetation ordination that follows the same west-east pollen-derived humidity pattern. Tree pollen (e.g. *Quercus ilex* and deciduous *Quercus*) abundances are higher in the eastern part of the AM where marine productivity is weaker. The CCA ordination as a function of marine environmental conditions reveals that pollen groups, such as open vegetation, Monocotyledonae, coastal vegetation, *Pinus*, human activity-related pollen taxa, Mediterranean forest, Eurosiberian forest, aquatic and mountainous region taxa, reflect a humidity gradient (Fig. 6). *Pinus* shows weaker concentrations at the AM sites than at the GoL ones. Except for *Pinus*, we suggest that wind-transported pollen to the AM area (Fig. 3b) is lower than hydrodynamic transport by runoff and river flows (including flash flood events) fostered by the open/clear ground vegetation.

Tree cover is lower in the AM catchment compared with the GoL and, conversely, there is a greater extent of open vegetation due to the semi-arid climate conditions. In Algeria, the degraded forest cover (Thornes et al., 1995) favours soil instability and erosional processes (Bouguerra et al., 2016). Flash flood events from autumn to spring (Arabi and Roose, 1989) represent up to 90% of the sedimentary input in the most erosion-sensitive AM areas (Benselama et al., 2021). Dissolved nutrients from erosional features are carried out to the sea by river flows. Strong occurrences of tree scattering or open vegetation then appear as a runoff signature.

The open vegetation pollen group in the AM study area is largely represented by Cichorioideae, Amaranthaceae and Poaceae, mainly typical of the open and/or coastal vegetation with their

xerophytous character and availability (due to their proximity) to be transported to the sea. Moreover, Cichorioideae are typical of the open landscapes and pastures, especially in the WMB in which they are commonly overrepresented (Florenzano et al., 2012; Florenzano et al., 2015) and associated with strong aridity (Jaouadi et al., 2010). The overrepresentation of xerophytous taxa in the AM (Fig. 2b) is coherent with the weaker precipitation regime in Algeria relative to the coastal GoL region (Maheras, 1988; González-Hidalgo et al., 2001) and the entire Rhône River catchment basin.

Semi-arid vegetation and Cupressaceae differ slightly from the main ordination pattern due to their altitudinal representation, implying higher concentrations around large oro-Mediterranean and alti-Mediterranean belt extensions. These zones are wider around the central to eastern part of the Tell Atlas due to higher altitudes.

The AM mountainous taxa group stands out from the other groups as it has only one representative taxon : *Cedrus*. These trees grow in the Atlas mountainous regions between 1300 and 2600 m, where there are relatively high precipitation rates between 500 and 2000 mm/year (Bentouati, 2008; Cheddadi et al., 2009). *Cedrus* is only observed in samples between 3°E and 5°E along the AM, which is consistent with its coastal watershed distribution in the highest part of the Tell Atlas. *Abies* and *Picea* are not represented in the AM, contrary to the GoL, due to higher temperatures and insufficient altitudes in the Tell Atlas compared with the Alps and Pyrenees mountains. Our pollen groups, therefore, clearly illustrate the robust link between pollen grain assemblages in the marine realm and vegetation on land, in agreement with studies focusing on a wider area of the WMB (Koreneva, 1971; Suc et al., 1989).

b. Contribution of continental NPP signatures to the analysis of marine sediments

Continental NPPs such as fungal, especially coprophilous (e.g. Shumilovskikh et al., 2021), spores suggest open or cleared ground landscapes favouring terrigenous input through their major runoff transport. Coprophilous spores can be interpreted as potential animal rearing or pastoralism indicators if supported with archaeological or palynological clues of human occupation in a continental context (e.g. Cugny et al., 2010; Montoya et al., 2018; Shumilovskikh et al., 2021). Coprophilous fungal spores, when identified as terrestrial species, can then be associated with the presence of herbivorous faeces in the adjacent catchments. However, correlations between human-related pollen taxa (i.e. agricultural activities on watersheds) and coprophilous spores is not detected in our results. Considering the broad diversity of marine fungal species, including coprophilous taxa originating from marine environments (Jones and Calabon, 1968; Richards et al., 2012; Jones et al., 2015; Jones et al.,

2019), and their occurrences even in deep sea environments (e.g. Raghukumar et al., 1992; Damare et al., 2006; Damare and Raghukumar, 2008), further studies are required to interpret these potential signals in marine sediments.

Glomus spores are mycorrhizal underground fungi spores that colonize higher terrestrial and aquatic plant roots (Jansonius and Kalgutkar, 2000; Schwarzott et al., 2001; Kohout et al., 2012), especially in lacustrine and fluvial environments (e.g. floodplains, van Geel et al., 1989; Shumilovskikh et al., 2016b; de Marins et al., 2017). *Glomus* can also be found on the coastline, especially in coastal dunes (Blaszowski and Czerniwska, 2011, Johansen et al., 2015; Stürmer et al., 2018) or tidal saltmarshes (Brown and Bledsoe, 1996). Also, it has been shown in continental studies that *Glomus* colonizes higher plant roots in arid to sub-arid contexts (e.g. Pande and Tarafdar, 2004; Anderson et al., 2011; Harikumar et al., 2015). In terrestrial contexts, this taxon is commonly interpreted as a tracer of erosional processes, depending on the type of substrate (Kolaczek et al., 2013), as supported by sedimentological and palynological signals (e.g. Anderson et al., 2011; Loughlin et al., 2018; Montoya et al., 2018). Higher *Glomus* occurrences in marine sediments may suggest stronger continental erosion, considering the large erosional sources of AM coastal *oueds*, linked to seasonal flash flood events. The high concentrations of *Glomus* in the AM sites (mean concentration of 540 spores/cm^3) compared with the GoL ones (mean concentration of 175 spores/cm^3) agree with the sparse forest cover in the AM, which leads to greater runoff and particle mobilisation. Nevertheless, to unambiguously connect marine occurrences of these fungi spores with erosional processes, notably in deep-sea sediments (Damare and Raghukumar, 2008), would require this signal to be crossed with other sedimentological or palynological proxies.

c. Land-sea synthesis in the newly studied Mediterranean areas

Our study underlines marked contrasts between pollen assemblages from the GoL and those from the AM, in response to north-south climatic gradients in precipitation and temperature, as reflected by the forest vs. subarid to steppic vegetation (Fig. 7). First, the latitudinal disparity between the two studied zones involves different atmospheric forcing such as mean atmospheric temperature (higher in the AM) and precipitation (higher in the GoL), directly linked with major atmospheric current patterns as outlined in the introduction of this paper. These gradients determine the characteristic vegetation belt extensions around the different studied zones.

The AM extends along a west to east gradient of increasing precipitation characterised by a decreasing representation of open vegetation and xerophytic pollen taxa (Figs. 1a, 2b and 3b).

Tree cover is much higher in the GoL compared with the AM and is associated with a higher representation of meso-Mediterranean compared with thermo-Mediterranean (e.g. more *Quercus ilex* at the expense of *Olea*) taxa in the pollen spectra (Figs. 2b and 3b). The GoL, despite a high representation of the Eurosiberian tree pollen due to high precipitation, shows a high pollen diversity due to the size of the combined regional river and Rhône River catchment basins. This influence is obvious through an inshore-offshore pattern of both pollen and dinocyst distributions.

Pollen of mountain *Abies* and *Picea* taxa are exclusively transported by river discharge into the GoL marine sediments (Beaudoin et al., 2007). The Rhône River watershed covers large mountainous areas from the Alps, which is the only area where *Picea* is found, to the Pyrenees and adjacent mountains of southern France (e.g. Montagne Noire, Cevennes, Corbières) where *Abies* is found. All the other taxa reflect the regional vegetation of the GoL, with a strong representation of the Mediterranean taxa advected from the coastal watersheds and nearby areas as previously shown by Beaudoin et al. (2007). Pollen grains are mainly transported by rivers to the GoL shelf sediments and, except for *Pinus*, their distribution on the shelf has been shown not to be affected by potential sorting by the current circulations (Beaudoin et al., 2007).

Coastal vegetation, Cupressaceae, semi-arid vegetation, mountainous region vegetation, Mediterranean forest, Eurosiberian forest, Monocotyledonae (mainly representing open and hydrophytous vegetation), aquatic plants, open vegetation, human activity-related pollen and trilete spore concentrations are higher in estuarine conditions than further out at sea and reflect the diversity of environments being drained on the catchment basins of the GoL.

The pollen data from the AM demonstrates vegetation and hydrological gradients, both of which are linked to Atlantic influences (such as the MAW) that decrease from west to east. These gradients are characterised by: i) a decreasing amount of MAW flow within the AC and an easterly weakening of the density front, and ii) an increase in moisture supply in the eastern part of the AM, where Atlantic stormy events occur frequently, guided by the Mediterranean storm track. Indeed, most of the south-western WMB is rarely crossed by the storm tracks driving precipitation (Lionello et al., 2016), compared with the north-eastern part of Algeria and north of Tunisia. This atmospheric configuration results in greater dryness in the western part of the AM, favouring xerophytic plants, and more moisture on the north African coast of eastern Algeria and Tunisia, favouring sclerophytous plants (Figs. 2b and 3b). Pollen levels of Eurosiberian forest trees, aquatic plant and mountainous taxa (as well as freshwater algae and trilete spores) indicate reduced wet zones around annual water flowing rivers or seasonal lakes (aquatic plants) and higher altitudes (Eurosiberian and mountainous vegetation). Thus, despite

gradually increasing precipitation eastward of 3°E, river discharge and associated productivity conditions in western and central Algeria are lower than those in the wetter eastern part of the AM. This observation suggests that the MAW-derived upwelling front is the major productivity driver in the AM.

6. Conclusion

We document zonal disparities in marine and continental palynomorph distributions in two major productive areas of the mostly oligotrophic western Mediterranean Basin (WMB). i) The Gulf of Lion (GoL) productive pattern combines nutrient-enriched river discharge mainly driven by the Rhône River and seasonal coastal upwelling cells due to the combined effect of the Mistral and Tramontane winds. ii) The Algerian Margin (AM) productivity pattern is mainly supported by upwelling cells along the surface water density front due to the inflow of the Modified Atlantic Waters along the Algerian Current (AC) and intense sporadic seasonal river discharge and runoff on the northern African coast. Our results document areas not covered by the published WMB modern dinocyst database, and enlarge its coverage to n = 102 sites. We illustrate the strong sensitivity of dinocyst assemblages to mesoscale climatic forcing, suggesting that the vigour of the MAW inflow directly impacts the AC and related dinocyst-derived productivity, as inferred from the distribution of *Brigantedinium* spp. in the WMB. We also show an obvious link between continental palynomorph distributions in both marine studied sites with climate on the adjacent continent and hydrological conditions inferred from dinocyst assemblages. Pollen distribution in the marine realm also reflects the climatic and geomorphological conditions of the northern vs. southern WMB, showing strong dependence on the distribution of the vegetation belts within the GoL and AM watersheds. For example, the extent of forest and its partition between Mediterranean and Eurosiberian taxa are strongly controlled by precipitation regimes and reflect the moister northern GoL and drier southern AM regions. We also suggest that continental non-pollen palynomorphs, especially those of the fungal *Glomus* type, could constitute a good bio-indicator of soil erosion when high occurrences are recorded in marine sediments.

7. Acknowledgments

This work was part of a PhD thesis (Coussin V.) financed by the *Région Bretagne* and UBO (University of Brest). This work was supported by the French national programme (CNRS) LEFE-EC2CO ('DATAPOL'), by the 'ISblue' project (Interdisciplinary graduate school for the blue planet; ANR-17-EURE-0015), and was co-funded by a grant from the French government under the program *Investissements d'Avenir*. We thank the captains, crews and scientific teams of the cruises that collected studied cores: GMO1 (Pierre Cochonat, Bernard Dennielou), GMO2-CARNAC (Nabil Sultan, Michel Voisset), BEACHMED (Catherine Satra Le Bris) and RHOSOS (Serge Berné, Bernard Dennielou). We also thank the Ifremer for access to the sedimentology laboratory and Marion Genet for the sample sharing. We acknowledge the ANR BRAISE project, grant ANR-19-CE01-0001-01, for the funding of the $^{210}Pb_{xs}$ measurements of the Gulf of Lion sediments. We thank Yannick Miras for his help with the determination of non-pollen palynomorphs and discussion about their ecological signature. We would like to thank the *Bureau de traduction* of the University of Brest for the improvement of English, and the two reviewers for their constructive and precise comments.

8. Data availability

All data discussed in the manuscript are available in the SEANOE repository: Coussin Vincent, Penaud Aurelie, Combourieu-Nebout Nathalie, Peyron Odile, Schmidt Sabine, Zaragosi Sebastien, de Vernal Anne, Babonneau Nathalie (2022). Distribution of modern dinocysts and pollen in the western Mediterranean Sea (Algerian Margin and Gulf of Lion). SEANOE. https://doi.org/10.17882/87317

9. Table

Table 1: List of the 25 study samples with their collection cruise and geographical information.

Age ranges of top core samples are given when available, based on radionuclide analyses.

Table 1
List of the 25 study samples with their collection cruise and geographical information. Age ranges of top core samples are given when available, based on radionuclide analyses.

Cruise	Year	Core	OBS (cm)	Latitude (°N)	Longitude (°E)	Depth (m)	Lithology	Age range	Reference of dating
PRISME	2007	PSM-KS19	0–1.5	36.63	0.29	2624	Mud	60 < T < 100 yrs	this study
PRISME	2007	PSM-KS20	0–1	36.80	0.62	2652	Mud	100 < *T* < 200 yrs	this study
PRISME	2007	PSM-KS30	0–1	37.19	3.34	2769	Mud	No date	
PRISME	2007	PSM-KS33	0–1	36.80	3.50	104	Sandy mud	*T* < 60 yrs	this study
PRISME	2007	PSM-KS34	0.5–2	36.82	3.54	137	Sandy mud	T < 60 yrs	this study
PRISME	2007	PSM-KS35	0–1	36.81	3.49	131	Sandy mud	T < 60 yrs	this study
MARADJA	2003	IMDJ03	0–0.5	36.95	3.29	2431	Mud	No date	
MARADJA2	2005	IMDJ12	0–1	37.00	3.79	1650	Mud	No date	
MARADJA2	2005	IMDJ25	0–0.5	36.46	0.42	2354	Mud	30 < T < 60 yrs	this study
MARADJA	2003	KMDJ07	0–1	36.54	0.13	2624	Mud	100 < T < 200 yrs	this study
MARADJA2	2005	KMDJ13	0–1	37.03	3.77	2158	Mud	No date	
MARADJA2	2005	KMDJ19	0–0.5	36.96	3.19	2473	Mud	60 < T < 100 yrs	Genet (2022)
MARADJA2	2005	KMDJ20	0–0.5	36.98	3.33	2343	Mud	100 < T < 200 yrs	Genet (2022)
MARADJA2	2005	KMDJ22	0–0.5	36.48	0.47	2098	Mud	30 < T < 60 yrs	this study
MARADJA2	2005	KMDJ23	0–0.5	36.50	0.26	2542	Mud	30 < T < 60 yrs	this study
MARADJA2	2005	KMDJ24	0–0.5	36.47	0.42	2354	Mud	30 < T < 60 yrs	this study
MARADJA2	2005	KMDJ29	0–0.5	36.91	2.67	616	Mud	No date	
MARADJA2	2005	KMDJ36	0–1	37.13	5.36	2462	Mud	No date	
MARADJA2	2005	KMDJ38	0–1	37.22	8.00	1015	Mud	T < 60 yrs	this study
GMO2-CARNAC	2002	KIGC 01	0–0.5	41.92	4.71	2435	Mud	T < 20 yrs	Genet (2022)
BEACHMED	2004	BM-KS12	0–0.5	43.44	4.02	29	Mud	60 < *T* < 100 yrs	Genet (2022)
RHOSOS	2008	RHS-KS39	0–0.5	43.38	4.51	20	Sandy mud	20 < T < 60 yrs	Genet (2022)
RHOSOS	2008	RHS-KS51	0–0.5	43.27	4,92	89	Sandy mud	20 < T < 60 yrs	Genet (2022)
GMO1	2001	KGMO-10	0–0.5	42.26	4.78	2066	Mud	T < 20 yrs	Genet (2022)
GMO1	2001	KGMO-14	0–0.5	42.78	3.67	234	Sand	100 < T < 200 yrs	Genet (2022)

10. Figures

Fig. 1. Maps presenting characteristics of the western Mediterranean Basin (WMB): a) sea surface temperature, and major sea surface and atmospheric currents (simplified vegetation cover is shown according to Beaudoin et al., 2007, and Tassin, 2012); b) sea surface chlorophyll-a concentration, annual primary productivity (green circles) of each study site and major rivers flowing into the WMB; c) the new studied sites (white dots) and modern dinocyst database sites (black dots) extracted from de Vernal et al. (2020).

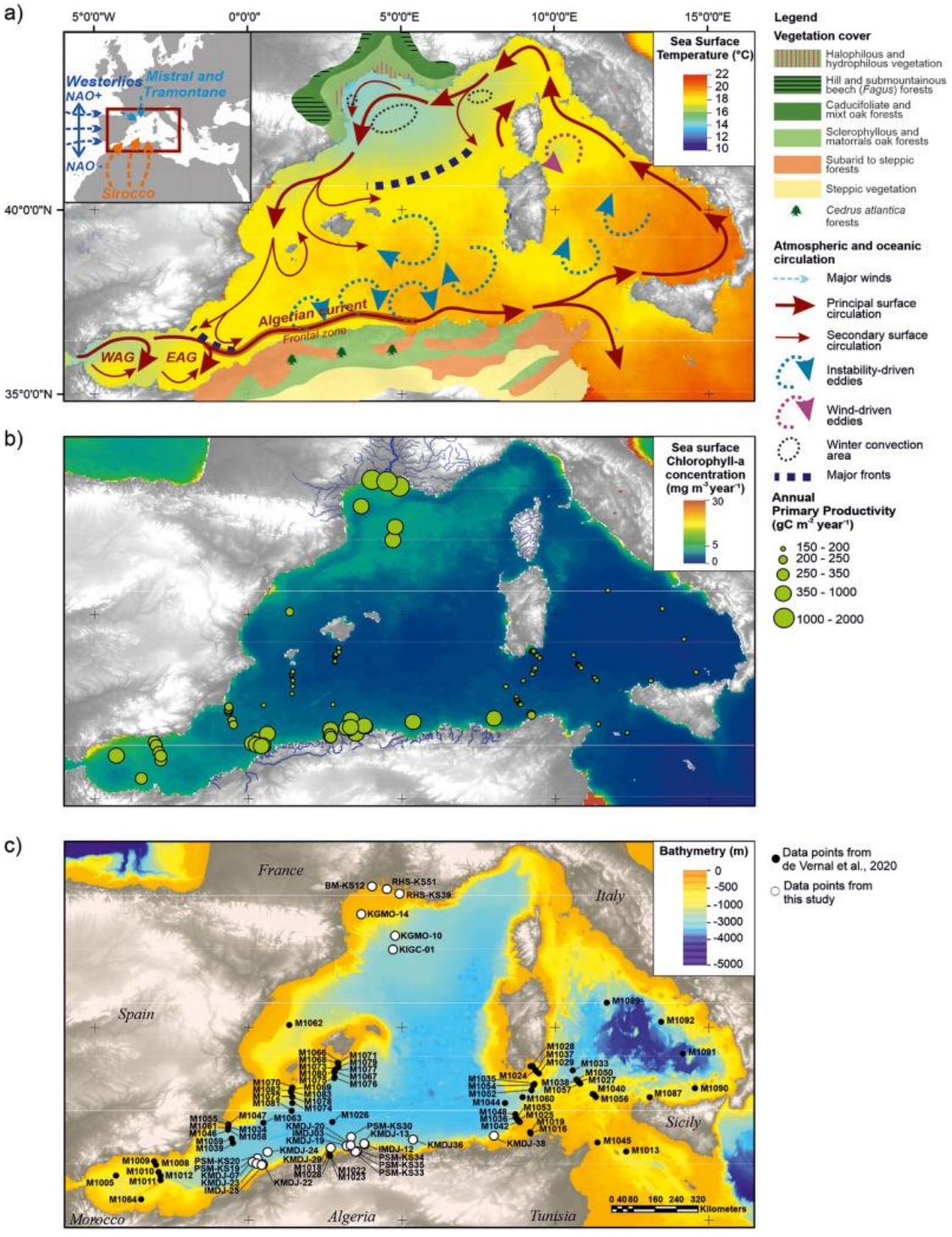

Fig. 2. a) Dinocyst diagram (percentages of selected taxa with values exceeding 1% at least once among the studied samples) for the Gulf of Lion (blue labels) and Algerian Margin (red labels), with related ecological groups. Dinocyst zones are based on a CONISS statistical analysis. b) Pollen diagram (percentages of selected taxa exceeding 1% in all studied samples, when *Pinus* is excluded from the main pollen sum) for the studied sites in the Gulf of Lion and Algerian Margin, with related ecological groups. Continental non-pollen palynomorphs (NPP) are highlighted in percentages and calculated based on a sum including total pollen (without *Pinus*) and continental NPP counts.

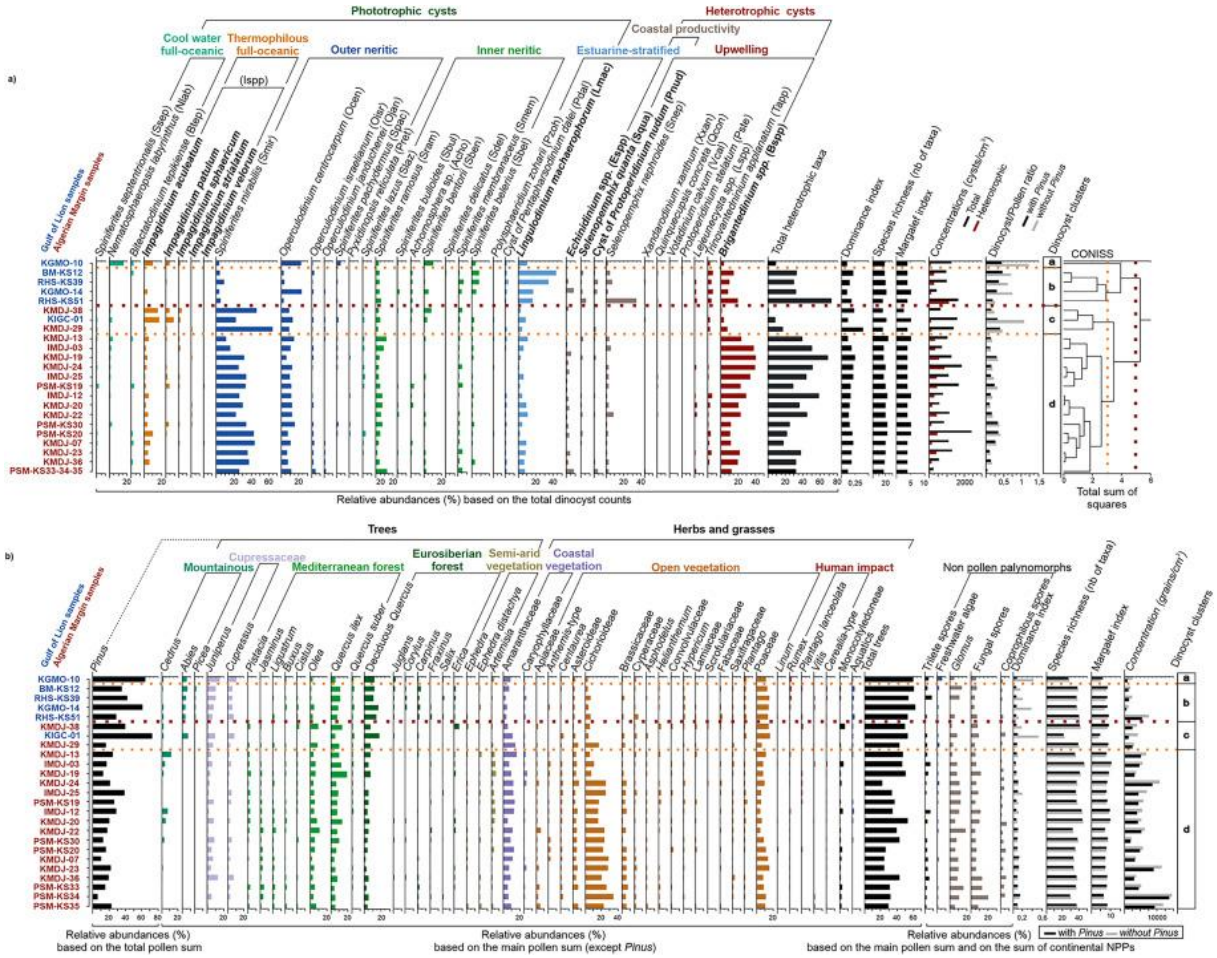

Fig. 3. a) Distribution maps of selected dinocyst results for the Gulf of Lion and Algerian Margin. b) Distribution maps of selected pollen results for the Gulf of Lion and Algerian Margin. Here, pollen percentages are calculated for all taxa on a basis of the total pollen count, *Pinus* included.

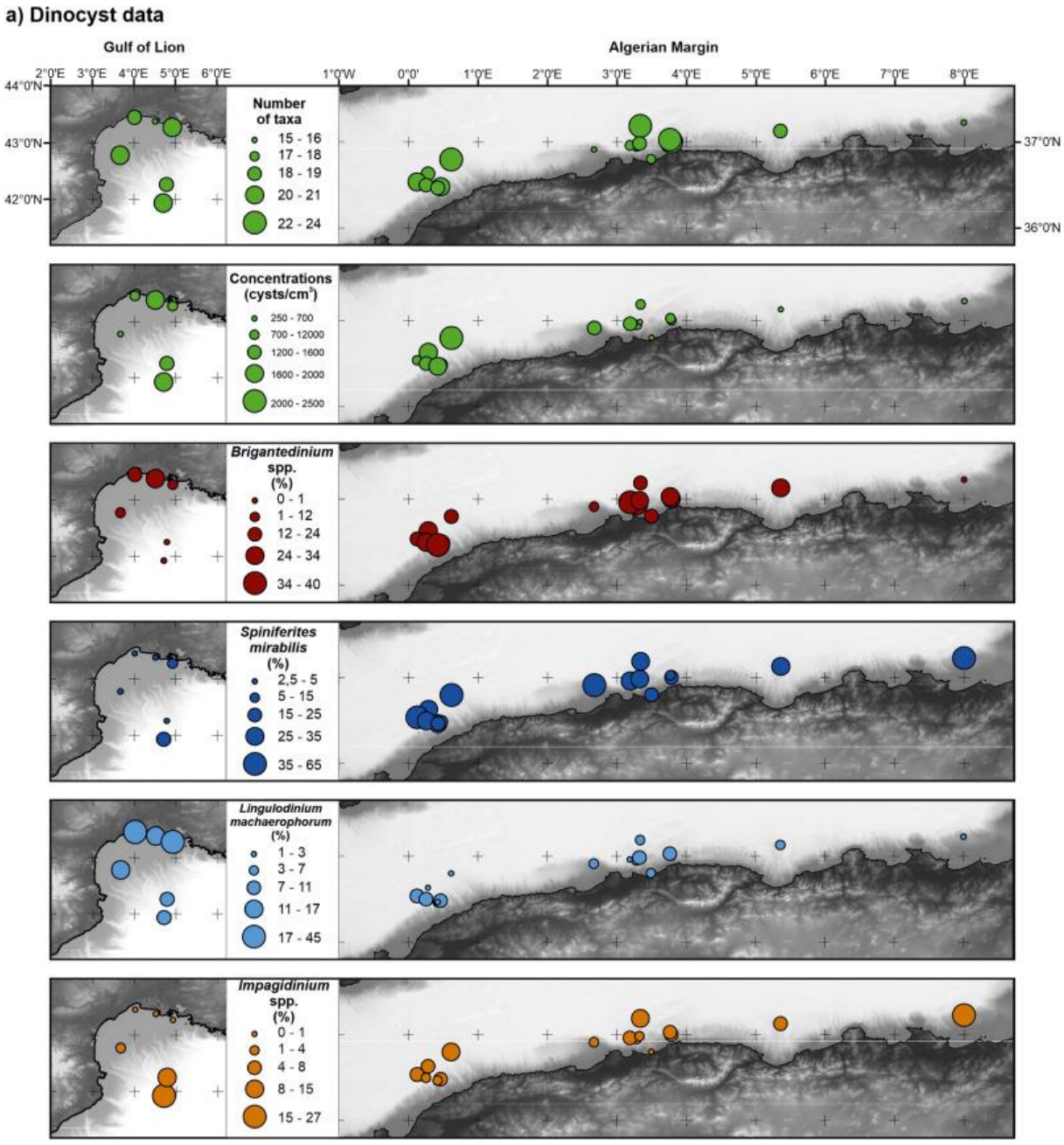

Fig. 4. a) Detrended correspondence analysis (DCA) based on dinocyst assemblages (percentages) of the 23 new study samples combined with the 79 sites in the modern dinocyst database for the western Mediterranean Basin (de Vernal et al., 2020). b) Canonical correspondence analysis (CCA) based on dinocyst assemblages (percentages) of the enlarged modern dinocyst database for the WMB (n = 102 sites) cross-referenced with environmental parameters (see Materials and Methods section). Dinocyst taxa are abbreviated according to the codes noted in Fig. 2a. Dcoast: distance to the coast, SSS winter and SSS summer: winter and summer sea surface salinity, SST winter and SST summer: winter and summer sea surface temperature, PP annual: annual primary productivity (in gC m^2 $year^{-1}$), DO: Dissolved Oxygen (ml/l), N: nitrate concentration (µmol/l), P: phosphate concentration (µmol/l), Si: silicate concentration (µmol/l). c) Canonical correspondence analysis (CCA) based on dinocyst assemblages (percentages) for the Algerian Margin study samples (n = 17 sites) as a function of environmental parameters. For both CCA, 22 dinocyst taxa were selected. Dinocyst taxa code denomination is the same as that used in Fig. 4.b Dinocyst taxa are abbreviated in the same way as in the dinocyst diagram taxa headers (Fig. 2a).

a) DCA modern Western Mediterranean dinocysts assemblages (n=102)

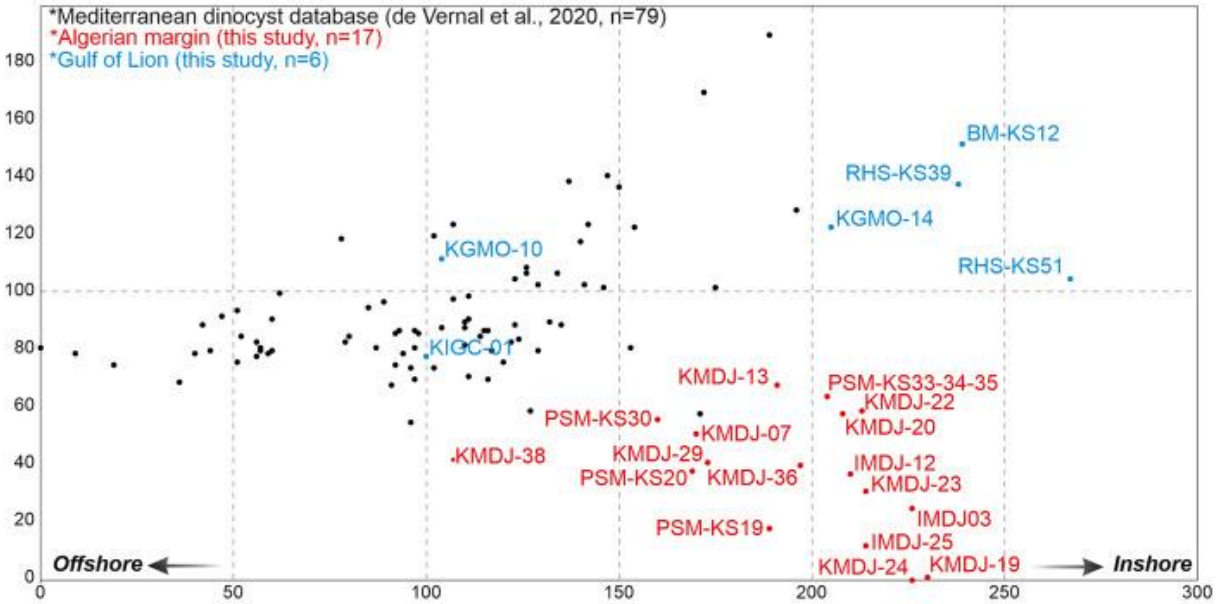

b) CCA on dinocyst taxa (%) - Western Mediterranean sites (n=102)

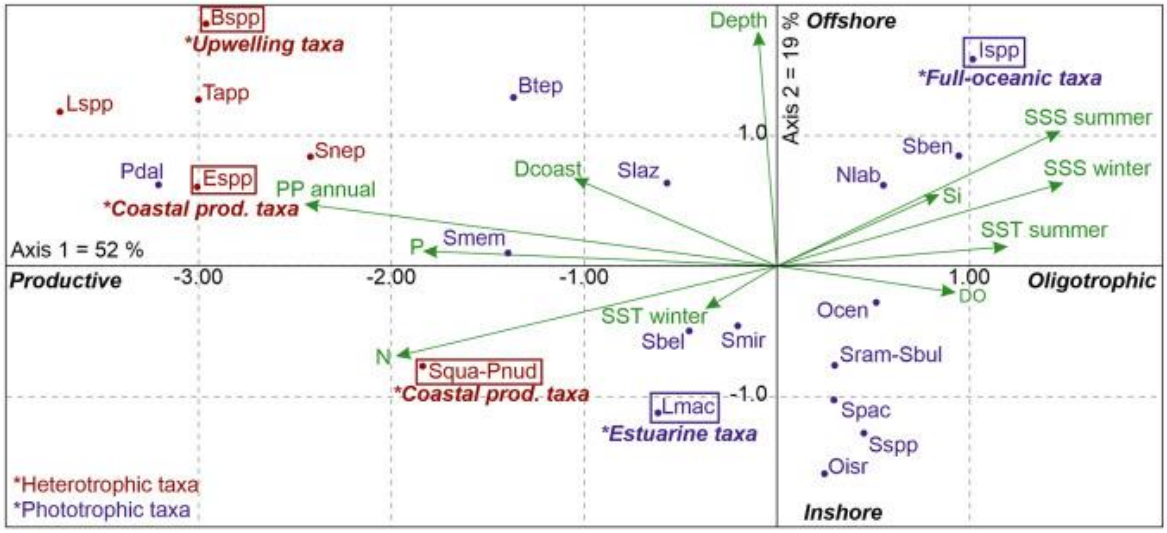

c) CCA on dinocyst taxa (%) - Algerian margin sites (n=17)

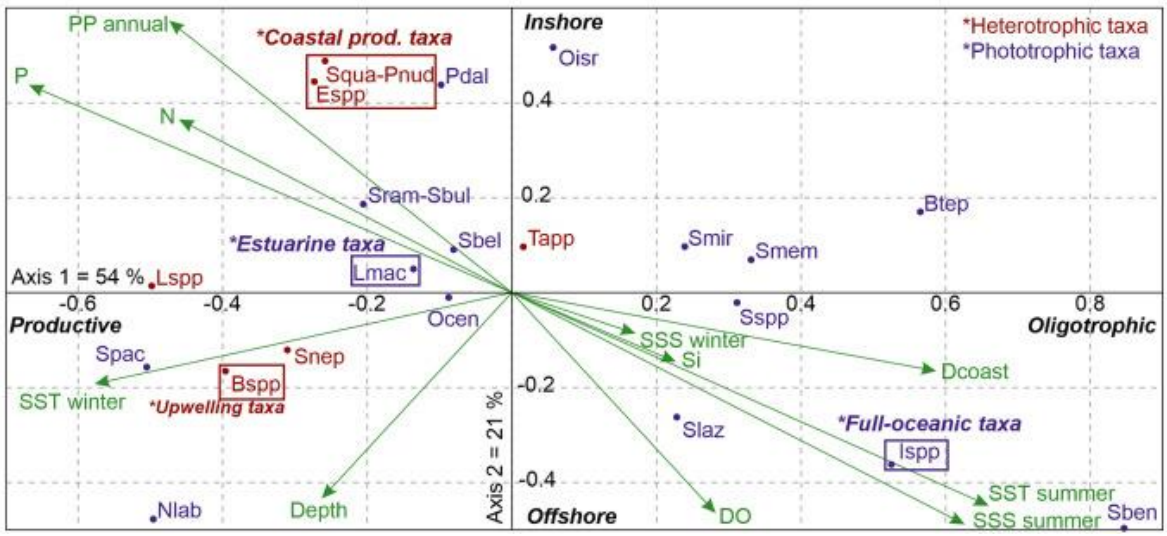

Fig. 5. Results from the new study sites (green circles) and sites from the modern dinocyst database of de Vernal et al., 2020 (red circles) for a) dinocyst species richness (i.e. number of different taxa), and relative abundances of: b) heterotrophic taxa, c) *Brigantedinium* spp., d) miscellaneous peridinioid cysts or 'MPC' (*Lejeunecysta* spp., *Selenopemphix nephroides, Quinquecupsis concreta, Votadinium calvum, Trinovantedninium applanatum*, *Stelladinium stellatum, Selenopemphix quanta*, *Protoperidinium nudum*), and e) cold water taxa (*Bitectatodinium tepikiense, Nematosphaeropsis labyrinthus*, *Spiniferites lazus*), f) *Spiniferites mirabilis*, g) *Impagidinium* spp., h) *Operculodinium* spp., i) Coastal productivity taxa (*Echinidinium* spp., *Selenopemphix quanta* and cysts of *Protoperidinium nudum)* and, j) *Lingulodinium machaerophorum.*

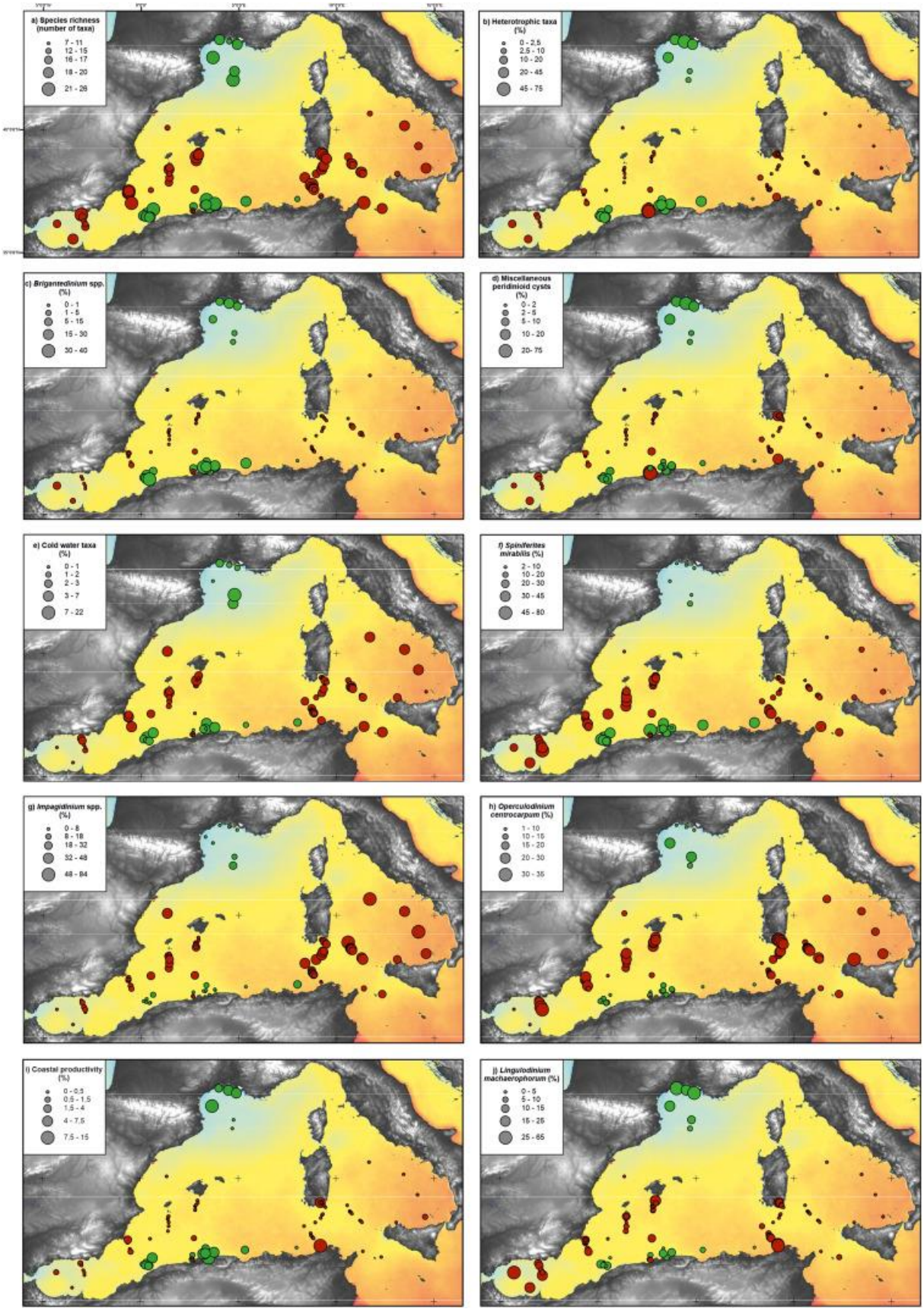
a) Species richness (number of taxa)
7 - 11
12 - 15
16 - 17
18 - 20
21 - 28
b) Heterotrophic taxa (%)
0 - 2.5
2.5 - 10
10 - 20
20 - 45
45 - 75
c) Brigantedinium spp. (%)
0 - 1
1 - 5
5 - 15
15 - 30
30 - 40
d) Miscellaneous peridinioid cysts (%)
0 - 2
2 - 5
5 - 10
10 - 20
20- 75
e) Cold water taxa (%)
0 - 1
1 - 2
2 - 3
3 - 7
7 - 22
f) Spiniferites mirabilis (%)
2 - 10
10 - 20
20 - 30
30 - 45
45 - 80
g) Impagidinium spp. (%)
0 - 8
8 - 18
18 - 32
32 - 48
48 - 84
h) Operculodinium centrocarpum (%)
1 - 10
10 - 15
15 - 20
20 - 30
30 - 35
i) Coastal productivity (%)
0 - 0.5
0.5 - 1.5
1.5 - 4
4 - 7.5
7.5 - 15
j) Lingulodinium machaerophorum (%)
0 - 5
5 - 10
10 - 15
15 - 25
25 - 65

Fig. 6. Canonical correspondence analysis (CCA) based on log of pollen and continental non-pollen palynomorph (NPP) absolute concentrations (cysts/cm^3) for the Algerian Margin study samples (n = 13 sites). CCA environmental variables consist in dinocyst/pollen ratio, selected dinocyst and environmental parameters. Pollen and NPP groups are constituted according to the palynological diagram pollen taxa headers (Fig. 2b).

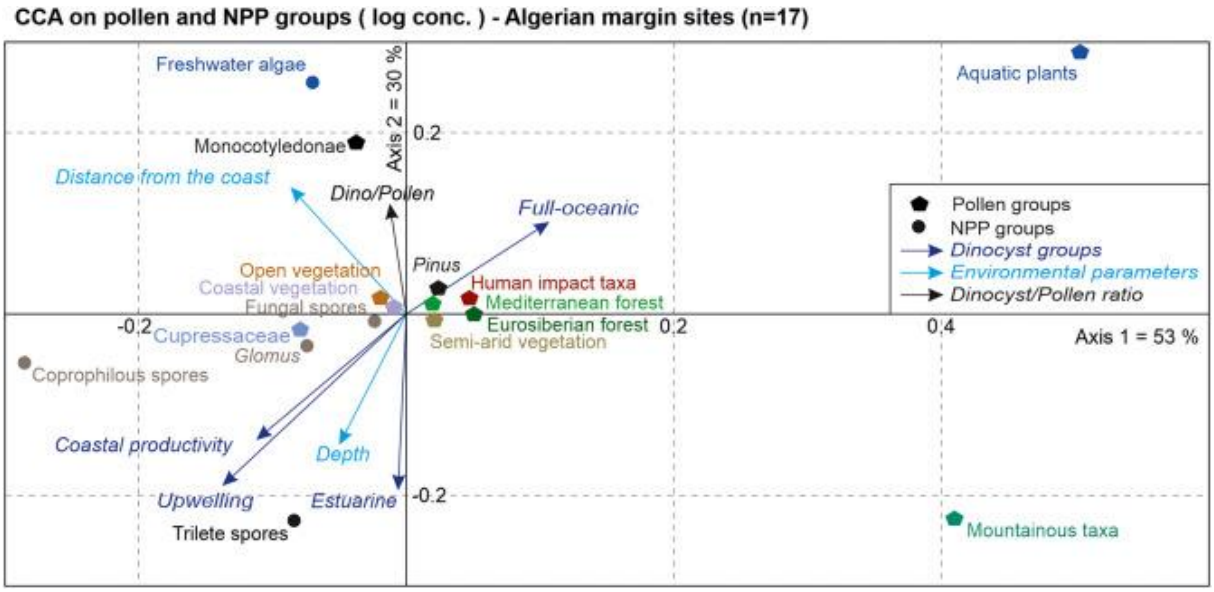

Fig. 7. Synoptical maps of major hydrographic features, sea surface and atmospheric currents in a) the Gulf of Lion and b) the Algerian margin. For both maps, main palynological information regarding dinocysts and pollen grains analysed in this study allows major gradients in palynomorph distribution to be considered in relation to our knowledge of oceanic features and vegetation cover in northern and southern Mediterranean watersheds.

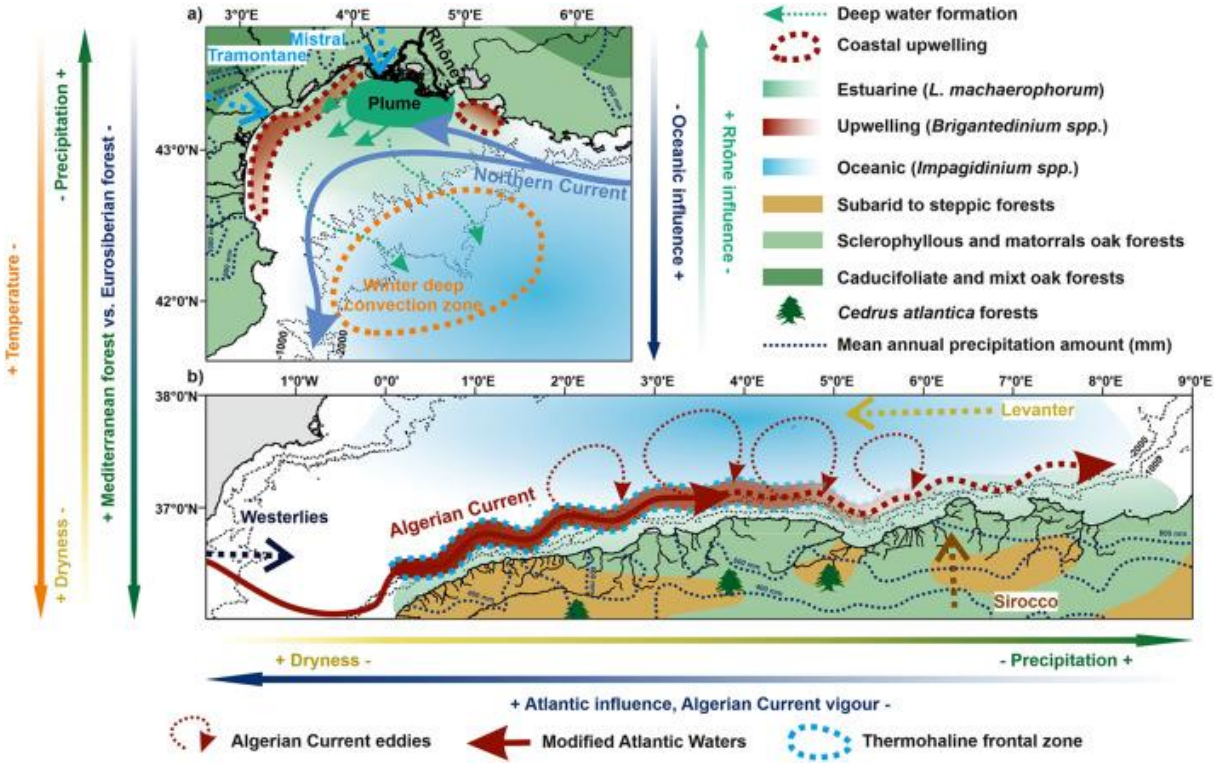

11. References

Aloisi, J., Jc, A., H, G., A, Maldonado, A, Monaco, 1979. Styles structuro-sédimentaires des marges continentales de la Méditerranée Nord-Occidentale.

Arabi, M., Roose, E., 1989. Influence du système de production et du sol sur l'érosion et le ruissellement en nappe en milieu montagnard méditerranéen (station d'Ouzera en Algérie). Bulletin-Réseau Erosion 39–51.

Arnone, R.A., Violette, P.E.L., 1986. Satellite definition of the bio-optical and thermal variation of coastal eddies associated with the African Current. Journal of Geophysical Research: Oceans 91, 2351–2364. https://doi.org/10.1029/JC091iC02p02351

Arnone, R.A., Wiesenburg, D.A., Saunders, K.D., 1990. The origin and characteristics of the Algerian Current. Journal of Geophysical Research: Oceans 95, 1587–1598. https://doi.org/10.1029/JC095iC02p01587

Bakun, A., Agostini, V.N., 2001. Seasonal patterns of wind-induced upwelling/downwelling in the Mediterranean Sea. scimar 65, 243–257. https://doi.org/10.3989/scimar.2001.65n3243

Barbéro, M., Quézel, P., Rivas-Martínez, S., 1981. Contribution à l'étude des groupements forestiers et préforestiers du Maroc. Phytocoenologia 311–412. https://doi.org/10.1127/phyto/9/1981/311

Bárcena, M.A., Flores, J.A., Sierro, F.J., Pérez-Folgado, M., Fabres, J., Calafat, A., Canals, M., 2004. Planktonic response to main oceanographic changes in the Alboran Sea (Western Mediterranean) as documented in sediment traps and surface sediments. Marine Micropaleontology 53, 423–445. https://doi.org/10.1016/j.marmicro.2004.09.009

Beaudouin, C., Suc, J.-P., Escarguel, G., Arnaud, M., Charmasson, S., 2007. The significance of pollen signal in present-day marine terrigenous sediments: The example of the Gulf of Lions (western Mediterranean Sea). Geobios 40, 159–172. https://doi.org/10.1016/j.geobios.2006.04.003

Benabid, A., 1982. Bref aperçu sur la zonation altitudinale de la végétation climacique du Maroc. Ecologia Mediterranea 8, 301–315. https://doi.org/10.3406/ecmed.1982.1956

Benselama, O., Hasbaia, M., Djoukbala, O., Boutaghane, H., Ferhati, A., Djerbouai, S., 2021. Suspended sedimentary dynamics under Mediterranean semi-arid environment of Wadi El Maleh watershed, Algeria. Modeling Earth Systems and Environments. https://doi.org/10.1007/s40808-021-01133-4

Bentouati, A., 2008. La situation du cèdre de l'Atlas dans les Aurès (Algérie), in: Forêt méditerranéenne. Presented at the Changements climatiques et forêt méditerranéenne. Actes du colloque de novembre 2007, pp. 203–208.

Berland, B.R., Bonin, D.J., Guerin-Ancey, O., Antia, N.J., 1979. Concentration requirement of glycine as nitrogen source for supporting effective growth of certain marine microplanktonic algae. Marine Biology 55, 83–92.

Behoux, J.P., 1984. Paléo-hydrologie de la Méditerranée au cours des derniers 20 000 ans. Oceanologica acta 7, 43–48.

Bethoux, J.P., 1981. Le phosphore et l'azote en mer Mediterranee, bilans et fertilite potentielle. Marine Chemistry 10, 141–158. https://doi.org/10.1016/0304-4203(81)90029-3

Bethoux, J.P., 1979. Budgets of the Mediterranean Sea-Their dependance on the local climate and on the characteristics of the Atlantic waters. Oceanologica acta 2, 157–163.

Bethoux, J.P., Gentili, B., Morin, P., Nicolas, E., Pierre, C., Ruiz-Pino, D., 1999. The Mediterranean Sea: a miniature ocean for climatic and environmental studies and a key for the climatic functioning of the North Atlantic. Progress in Oceanography 44,

131–146.
Bethoux, J.P., Gentili, B., 1994. The Mediterranean Sea, a Test Area for Marine and Climatic Interactions, in: Malanotte-Rizzoli, P., Robinson, A.R. (Eds.), Ocean Processes in Climate Dynamics: Global and Mediterranean Examples, NATO ASI Series. Springer Netherlands, Dordrecht, pp. 239–254. https://doi.org/10.1007/978-94-011-0870-6_11
Biebow, N., 1996. Dinoflagellatenzysten als Indikatoren der spät-und postglazialen Entwicklung des Auftriebsgeschehens vor Peru (PhD Thesis). GEOMAR Forschungszentrum für marine Geowissenschaften der Christian.
Blaszkowski, J., Czerniawska, B., 2011. Arbuscular mycorrhizal fungi (Glomeromycota) associated with roots of Ammophila arenaria growing in maritime dunes of Bornholm (Denmark). Acta Societatis Botanicorum Poloniae 80.
Bos, J.A.A., Huisman, D.J., Kiden, P., Hoek, W.Z., van Geel, B., 2005. Early Holocene environmental change in the Kreekrak area (Zeeland, SW-Netherlands): A multi-proxy analysis. Palaeogeography, Palaeoclimatology, Palaeoecology 227, 259–289. https://doi.org/10.1016/j.palaeo.2005.05.020
Bouguerra, S., Bouanani, A., Baba-Hamed, K., 2016. Transport solide dans un cours d'eau en climat semi-aride : cas du bassin versant de l'Oued Boumessaoud (nord-ouest de l'Algérie). rseau 29, 179–195. https://doi.org/10.7202/1038923ar
Bouimetarhan, I., Marret, F., Dupont, L., Zonneveld, K., 2009. Dinoflagellate cyst distribution in marine surface sediments off West Africa (17–6 N) in relation to sea-surface conditions, freshwater input and seasonal coastal upwelling. Marine Micropaleontology 71, 113–130.
Brown, A.M., Bledsoe, C., 1996. Spatial and temporal dynamics of mycorrhizas in Jaumea carnosa, a tidal saltmarsh halophyte. Journal of Ecology 703–715.
Bryden, H.L., Kinder, T.H., 1991. Steady two-layer exchange through the Strait of Gibraltar. Deep Sea Research Part A. Oceanographic Research Papers 38, S445–S463.
Campbell, R., Diaz, F., Hu, Z., Doglioli, A., Petrenko, A., Dekeyser, I., 2013. Nutrients and plankton spatial distributions induced by a coastal eddy in the Gulf of Lion. Insights from a numerical model. Progress in Oceanography 109, 47–69.
Cheddadi, R., Fady, B., François, L., Hajar, L., Suc, J.-P., Huang, K., Demarteau, M., Vendramin, G.G., Ortu, E., 2009. Putative glacial refugia of Cedrus atlantica deduced from Quaternary pollen records and modern genetic diversity. Journal of Biogeography 36, 1361–1371. https://doi.org/10.1111/j.1365-2699.2008.02063.x
Coste, B., 1974. Role of the Mineral Nutrients Contributed by the River Rhone(France) to the Organic Production of the Waters of the Gulf of Lions,(In French). Tethys 6 (4) p 727-740, 1974.
Coussin, V., 2021. Gradients climatiques continentaux et hydrologiques au cours de l'Holocène dans la marge Algérienne au Golfe du Lion : approche multi-proxy (palynologie, sédimentologie, biomarqueurs moléculaires et reconstructions climatiques). PhD Univ Brest, 369 pp.
Cugny, C., Mazier, F., Galop, D., 2010. Modern and fossil non-pollen palynomorphs from the Basque mountains (western Pyrenees, France): the use of coprophilous fungi to reconstruct pastoral activity. Veget Hist Archaeobot 19, 391–408. https://doi.org/10.1007/s00334-010-0242-6
Dale, B., Dale, A.L., Jansen, J.H.F., 2002. Dinoflagellate cysts as environmental indicators in surface sediments from the Congo deep-sea fan and adjacent regions. Palaeogeography, Palaeoclimatology, Palaeoecology 185, 309–338. https://doi.org/10.1016/S0031-0182(02)00380-2
Dale, B., Fjellså, A., 1994. Dinoflagellate Cysts as Paleoproductivity Indicators: State of the Art, Potential, and Limits, in: Zahn, R., Pedersen, T.F., Kaminski, M.A., Labeyrie, L.

(Eds.), Carbon Cycling in the Glacial Ocean: Constraints on the Ocean's Role in Global Change, NATO ASI Series. Springer, Berlin, Heidelberg, pp. 521–537. https://doi.org/10.1007/978-3-642-78737-9_22
Dale, B., Thorsen, T.A., Fjellsa, A., 1999. Dinoflagellate Cysts as Indicators of Cultural Eutrophication in the Oslofjord, Norway. Estuarine, Coastal and Shelf Science 48, 371–382. https://doi.org/10.1006/ecss.1999.0427
Damare, S., Raghukumar, C., 2008. Fungi and macroaggregation in deep-sea sediments. Microbial Ecology 56, 168–177.
Damare, S., Raghukumar, C., Raghukumar, S., 2006. Fungi in deep-sea sediments of the Central Indian Basin. Deep Sea Research Part I: Oceanographic Research Papers 53, 14–27.
de Marins, J.F., Carrenho, R., Thomaz, S.M., 2009. Occurrence and coexistence of arbuscular mycorrhizal fungi and dark septate fungi in aquatic macrophytes in a tropical river–floodplain system. Aquatic Botany 91, 13–19.
de Marins, J. F., & Carrenho, R., 2017. Arbuscular mycorrhizal fungi and dark septate fungi in plants associated with aquatic environments. Acta Botanica Brasilica, 31, 295-308.
de Vernal, A., Henry, M., Bilodeau, G., 1999. Techniques de préparation et d'analyse en micropaléontologie. Les cahiers du GEOTOP 3, 41.
de Vernal, A., Radi, T., Zaragosi, S., Van Nieuwenhove, N., Rochon, A., Allan, E., De Schepper, S., Eynaud, F., Head, M.J., Limoges, A., Londeix, L., Marret, F., Matthiessen, J., Penaud, A., Pospelova, V., Price, A., Richerol, T., 2020. Distribution of common modern dinoflagellate cyst taxa in surface sediments of the Northern Hemisphere in relation to environmental parameters: The new n=1968 database. Marine Micropaleontology, Taxonomy and distribution of modern organic-walled dinoflagellate cysts in surface sediments from the Northern Hemisphere: an update of Rochon et al., 1999 159, 101796. https://doi.org/10.1016/j.marmicro.2019.101796
Diaz, F., Raimbault, P., Conan, P., 2000. Small-scale study of primary productivity during spring in a Mediterranean coastal area (Gulf of Lions). Continental Shelf Research 20, 975–996.
Dünkeloh, A., Jacobeit, J., 2003. Circulation dynamics of Mediterranean precipitation variability 1948–98. International Journal of Climatology: A Journal of the Royal Meteorological Society 23, 1843–1866.
Esper, O., Zonneveld, K.A.F., 2007. The potential of organic-walled dinoflagellate cysts for the reconstruction of past sea-surface conditions in the Southern Ocean. Marine Micropaleontology 65, 185–212. https://doi.org/10.1016/j.marmicro.2007.07.002
Estournel, C., Kondrachoff, V., Marsaleix, P., Vehil, R., 1997. The plume of the Rhone: numerical simulation and remote sensing. Continental Shelf Research 17, 899–924. https://doi.org/10.1016/S0278-4343(96)00064-7
Fatela, F., Taborda, R., 2002. Confidence limits of species proportions in microfossil assemblages. Marine Micropaleontology 45, 169–174. https://doi.org/10.1016/S0377-8398(02)00021-X
Fensome, R.A., 1993. A classification of living and fossil dinoflagellates. Micropaleontology, special publication 7, 1–351.
Fieux, M., M, F., 1974. Formation d'eau dense sur le plateau continental du Golfe du Lion. Presented at the Processus de formation des eaux océaniques profondes en particulier Méditerranée occidentale, Paris, France, pp. 165–174.
Florenzano, A., Marignani, M., Rosati, L., Fascetti, S., Mercuri, A.M., 2015. Are Cichorieae an indicator of open habitats and pastoralism in current and past vegetation studies? Plant Biosystems - An International Journal Dealing with all Aspects of Plant Biology 149, 154–165. https://doi.org/10.1080/11263504.2014.998311

Florenzano, A., Torri, P., Rattighieri, E., N'Siala, I.M., Mercuri, A.M., 2012. Cichorioideae-Cichorieae as pastureland indicator in pollen spectra from southern Italy 12.
Galeron, M.-A., Amiraux, R., Charriere, B., Radakovitch, O., Raimbault, P., Garcia, N., Lagadec, V., Vaultier, F., Rontani, J.-F., 2015. Seasonal survey of the composition and degradation state of particulate organic matter in the Rhône River using lipid tracers. Biogeosciences 12, 1431–1446.
Ganne, A., Leroyer, C., Pénaud, A., Mojtahid, M., 2016. Present-day palynomorph deposits in an estuarine context: The case of the Loire Estuary. Journal of Sea Research 118, 35–51.
Garcia-Gorriz, E., Carr, M.-E., 2001. Physical control of phytoplankton distributions in the Alboran Sea: A numerical and satellite approach. Journal of Geophysical Research: Oceans 106, 16795–16805. https://doi.org/10.1029/1999JC000029
García-Herrera, R., Barriopedro, D., 2018a. Climate of the Mediterranean Region, in: Oxford Research Encyclopedia of Climate Science. Oxford University Press. https://doi.org/10.1093/acrefore/9780190228620.013.509
García-Herrera, R., Barriopedro, D., 2018b. Climate of the Mediterranean Region [WWW Document]. Oxford Research Encyclopedia of Climate Science. https://doi.org/10.1093/acrefore/9780190228620.013.509
Gaume, E., Borga, M., LLASSAT, M.C., Maouche, S., Lang, M., DIAKAKIS, M., 2016. Mediterranean extreme floods and flash floods, in: The Mediterranean Region under Climate Change. A Scientific Update, Coll. Synthèses. IRD Editions, pp. 133–144.
Gauthier, E., Bichet, V., Massa, C., Petit, C., Vannière, B., Richard, H., 2010. Pollen and non-pollen palynomorph evidence of medieval farming activities in southwestern Greenland. Vegetation History and Archaeobotany 19, 427–438.
Genet, M., 2022. Calibration du proxy microcharbon préservé dans les sédiments marins et reconstruction des paléo-incendies en région Méditerranéenne Occidentale au cours de l'Holocene. PhD Univ Bordeaux.
Giannakourou, A., Orlova, T.Y., Assimakopoulou, G., Pagou, K., 2005. Dinoflagellate cysts in recent marine sediments from Thermaikos Gulf, Greece: Effects of resuspension events on vertical cyst distribution. Continental Shelf Research 25, 2585–2596. https://doi.org/10.1016/j.csr.2005.08.003
Gilman, C., Garrett, C., 1994. Heat flux parameterizations for the Mediterranean Sea: The role of atmospheric aerosols and constraints from the water budget. Journal of Geophysical Research: Oceans 99, 5119–5134.
González-Hidalgo, J.C., Luis, M.D., Raventós, J., Sánchez, J.R., 2001. Spatial distribution of seasonal rainfall trends in a western Mediterranean area. International Journal of Climatology 21, 843–860. https://doi.org/10.1002/joc.647
Grimm, E., 1990. TILIA and TILIA.GRAPH: PC spreadsheet and graphics software for pollen data. INQUA Commission for the Study of the Holocene Working Group on Data Handling Methods Newsletter 4, 5–7.
Grimm, E., 1987a. CONISS: a FORTRAN 77 program for stratigraphically constrained cluster analysis by the method of incremental sum of squares. Computers & Geosciences 13, 13–35. https://doi.org/10.1016/0098-3004(87)90022-7
Grimm, E., 1987b. CONISS: A FORTRAN 77 program for stratigraphically constrained cluster analysis by the method of incremental sum of squares. Computers & Geosciences 13, 13–35. https://doi.org/10.1016/0098-3004(87)90022-7
Guizien, K., Charles, F., Lantoine, F., Naudin, J.-J., 2007. Nearshore dynamics of nutrients and chlorophyll during Mediterranean-type flash-floods. Aquat. Living Resour. 20, 3–14. https://doi.org/10.1051/alr:2007011
Hammer, O., Harper, D., Ryan, P., 2001. PAST: Paleontological Statistics Software Package

for Education and Data Analysis. Palaeontologia Electronica, Palaeontologia Electronica 4, 1–9.
Hammer, Ø., Harper, D.A., 2008. Paleontological data analysis. John Wiley & Sons.
Harikumar, V.S., Blaszkowski, J., Medhanie, G., Kanagaraj, M.K., Samuel, D.V., 2015. Arbuscular mycorrhizal fungi colonizing the plant communities in Eritrea, Northeast Africa. Applied Ecology and Environmental Research 13, 193–203.
Heusser, L.E., Balsam, W.L., 1985. Pollen sedimentation in the Northwest Atlantic: Effects of the Western Boundary Undercurrent. Marine Geology 69, 149–153. https://doi.org/10.1016/0025-3227(85)90138-0
Hurrell, J.W., 1995. Decadal Trends in the North Atlantic Oscillation: Regional Temperatures and Precipitation. Science 269, 676–679. https://doi.org/10.1126/science.269.5224.676
Hurrell, J.W., Kushnir, Y., Ottersen, G., Visbeck, M., 2003. An overview of the North Atlantic oscillation. Geophysical Monograph-American Geophysical Union 134, 1–36.
Jansonius, J., Kalgutkar, R.M., 2000. Redescription of some fossil fungal spores. Palynology 24, 37–47.
Jaouadi, S., Lebreton, V., Mulazzani, S., Boussofara, R., Mannai-Tayech, B., 2010. Analyses polliniques en contexte anthropisé: le cas du site holocène SHM-1 (Hergla, Tunisie centrale). Sezione di Museologia Scientifica e Naturalistica 6, 25–32.
Jiang, Q., Smith, R.B., Doyle, J., 2003. The nature of the mistral: Observations and modelling of two MAP events. Quarterly Journal of the Royal Meteorological Society 129, 857–875. https://doi.org/10.1256/qj.02.21
Johansen, R.B., Vestberg, M., Burns, B.R., Park, D., Hooker, J.E., Johnston, P.R., 2015. A coastal sand dune in New Zealand reveals high arbuscular mycorrhizal fungal diversity. Symbiosis 66, 111–121.
Johns, B., Marsaleix, P., Estournel, C., Véhil, R., 1992. On the wind-driven coastal upwelling in the Gulf of Lions. Journal of Marine Systems 3, 309–320. https://doi.org/10.1016/0924-7963(92)90008-V
Jones, E.G., Calabon, M., 1968. Marine fungi. Current Science 37, 378–379.
Jones, E.G., Pang, K.-L., Abdel-Wahab, M.A., Scholz, B., Hyde, K.D., Boekhout, T., Ebel, R., Rateb, M.E., Henderson, L., Sakayaroj, J., 2019. An online resource for marine fungi. Fungal Diversity 96, 347–433.
Jones, E.G., Suetrong, S., Sakayaroj, J., Bahkali, A.H., Abdel-Wahab, M.A., Boekhout, T., Pang, K.-L., 2015. Classification of marine ascomycota, basidiomycota, blastocladiomycota and chytridiomycota. Fungal Diversity 73, 1–72.
Koreneva, E.V., 1971. Spores and pollen in mediterranéen bottom sediments, in: The Micropalaeontology of Oceans: Proceedings of the Symposium Held in Cambridge from 10 to 17 September 1967 Under the Title'Micropalaeontology of Marine Bottom Sediments'. Cambridge University Press, p. 361.
Lacombe, H., Richez, C., 1982. The Regime of the Strait of Gibraltar, in: Nihoul, J.C.J. (Ed.), Elsevier Oceanography Series, Hydrodynamics of Semi-Enclosed Seas. Elsevier, pp. 13–73. https://doi.org/10.1016/S0422-9894(08)71237-6
Lamont, B., 1982. Mechanisms for enhancing nutrient uptake in plants, with particular reference to mediterranean South Africa and Western Australia. The Botanical Review 48, 597–689.
Lazzari, P., Solidoro, C., Salon, S., Bolzon, G., 2016. Spatial variability of phosphate and nitrate in the Mediterranean Sea: A modeling approach. Deep Sea Research Part I: Oceanographic Research Papers 108, 39–52. https://doi.org/10.1016/j.dsr.2015.12.006
Lewis, J., 1988. Cysts and Sediments: Gonyaulax Polyedra (Lingulodinium

Machaerophorum) in Loch Creran. Journal of the Marine Biological Association of the United Kingdom 68, 701–714. https://doi.org/10.1017/S0025315400028812
Lewis, J., Dodge, J., Powell, A., 1990. Quaternary dinoflagellate cysts from the upwelling system offshore Peru, Hole 686b, odp leg 1121, in: Proceedings of the Ocean Drilling Program, Scientific Results. pp. 323–328.
Lewis, J., Hallett, R., 1997. Lingulodinium polyedrum (Gonyaulax polyedra) a blooming dinoflagellate. Oceanography And Marine Biology: Volume 35 35, 89.
Lionello, P., Malanotte-Rizzoli, P., Boscolo, R., Alpert, P., Artale, V., Li, L., Luterbacher, J., May, W., Trigo, R., Tsimplis, M., 2006. The Mediterranean climate: an overview of the main characteristics and issues. Elsevier.
Lionello, P., Abrantes, F., Gacic, M., Planton, S., Trigo, R., Ulbrich, U., 2014. The climate of the Mediterranean region: research progress and climate change impacts. Reg Environ Change 14, 1679–1684. https://doi.org/10.1007/s10113-014-0666-0
Lionello, P., Trigo, I.F., Gil, V., Liberato, M.L.R., Nissen, K.M., Pinto, J.G., Raible, C.C., Reale, M., Tanzarella, A., Trigo, R.M., Ulbrich, S., Ulbrich, U., 2016. Objective climatology of cyclones in the Mediterranean region: a consensus view among methods with different system identification and tracking criteria. Tellus A: Dynamic Meteorology and Oceanography 68, 29391. https://doi.org/10.3402/tellusa.v68.29391
Lohrenz, S.E., Wiesenburg, D.A., DePalma, I.P., Johnson, K.S., Gustafson, D.E., 1988. Interrelationships among primary production, chlorophyll, and environmental conditions in frontal regions of the western Mediterranean Sea. Deep Sea Research Part A. Oceanographic Research Papers 35, 793–810. https://doi.org/10.1016/0198-0149(88)90031-3
Lolis, C.J., Bartzokas, A., Katsoulis, B.D., 2002. Spatial and temporal 850 hPa air temperature and sea-surface temperature covariances in the Mediterranean region and their connection to atmospheric circulation. International Journal of Climatology: A Journal of the Royal Meteorological Society 22, 663–676.
Lombo Tombo, S., Dennielou, B., Berné, S., Bassetti, M.-A., Toucanne, S., Jorry, S.J., Jouet, G., Fontanier, C., 2015. Sea-level control on turbidite activity in the Rhone canyon and the upper fan during the Last Glacial Maximum and Early deglacial. Sedimentary Geology 323, 148–166.
López-Moreno, J.I., Vicente-Serrano, S.M., Morán-Tejeda, E., Lorenzo-Lacruz, J., Kenawy, A., Beniston, M., 2011. Effects of the North Atlantic Oscillation (NAO) on combined temperature and precipitation winter modes in the Mediterranean mountains: Observed relationships and projections for the 21st century. Global and Planetary Change 77, 62–76. https://doi.org/10.1016/j.gloplacha.2011.03.003
Loughlin, N.J.D., Gosling, W.D., Montoya, E., 2018. Identifying environmental drivers of fungal non-pollen palynomorphs in the montane forest of the eastern Andean flank, Ecuador. Quaternary Research 89, 119–133. https://doi.org/10.1017/qua.2017.73
Maheras, P., 1988. Changes in precipitation conditions in the western mediterranean over the last century. Journal of Climatology 8, 179–189. https://doi.org/10.1002/joc.3370080205
Maheras, P., Xoplaki, E., Kutiel, H., 1999. Wet and dry monthly anomalies across the Mediterranean basin and their relationship with circulation, 1860–1990. Theoretical and Applied Climatology 64, 189–199.
Malanotte-Rizzoli, P., Robinson, A.R. (Eds.), 1994. Ocean Processes in Climate Dynamics: Global and Mediterranean Examples. Springer Netherlands, Dordrecht. https://doi.org/10.1007/978-94-011-0870-6
Margalef, Ramon, 1985. Environmental Control of the Mesoscale Distribution of Primary Producers and its Bearing to Primary Production in the Western Mediterranean, in:

Moraitou-Apostolopoulou, M., Kiortsis, V. (Eds.), Mediterranean Marine Ecosystems, NATO Conference Series. Springer US, Boston, MA, pp. 213–229. https://doi.org/10.1007/978-1-4899-2248-9_10
Margalef, Ramón, 1985. Primary production in upwelling areas. Energy, global ecology and resources. Producción primaria en áreas de afloramiento. Energía, ecología global y recursos.
Marret, F., 1994. Distribution of dinoflagellate cysts in recent marine sediments from the east Equatorial Atlantic (Gulf of Guinea). Review of Palaeobotany and Palynology 84, 1–22.
Marret, F., Bradley, L., de Vernal, A., Hardy, W., Kim, S.-Y., Mudie, P., Penaud, A., Pospelova, V., Price, A.M., Radi, T., Rochon, A., 2020. From bi-polar to regional distribution of modern dinoflagellate cysts, an overview of their biogeography. Marine Micropaleontology, Taxonomy and distribution of modern organic-walled dinoflagellate cysts in surface sediments from the Northern Hemisphere: an update of Rochon et al., 1999 159, 101753. https://doi.org/10.1016/j.marmicro.2019.101753
Marret, F., Zonneveld, K.A.F., 2003. Atlas of modern organic-walled dinoflagellate cyst distribution. Review of Palaeobotany and Palynology 125, 1–200. https://doi.org/10.1016/S0034-6667(02)00229-4
Médail, F., Quézel, P., 2003. Conséquences écologiques possibles des changements climatiques sur la flore et la végétation du bassin méditerranéen. Bocconea 16, 397–422.
Medail, F., Quezel, P., 1997. Hot-Spots Analysis for Conservation of Plant Biodiversity in the Mediterranean Basin. Annals of the Missouri Botanical Garden 84, 112–127. https://doi.org/10.2307/2399957
Mertens, K.N., Verhoeven, K., Verleye, T., Louwye, S., Amorim, A., Ribeiro, S., Deaf, A.S., Harding, I.C., De Schepper, S., González, C., Kodrans-Nsiah, M., De Vernal, A., Henry, M., Radi, T., Dybkjaer, K., Poulsen, N.E., Feist-Burkhardt, S., Chitolie, J., Heilmann-Clausen, C., Londeix, L., Turon, J.-L., Marret, F., Matthiessen, J., McCarthy, F.M.G., Prasad, V., Pospelova, V., Kyffin Hughes, J.E., Riding, J.B., Rochon, A., Sangiorgi, F., Welters, N., Sinclair, N., Thun, C., Soliman, A., Van Nieuwenhove, N., Vink, A., Young, M., 2009. Determining the absolute abundance of dinoflagellate cysts in recent marine sediments: The Lycopodium marker-grain method put to the test. Review of Palaeobotany and Palynology 157, 238–252. https://doi.org/10.1016/j.revpalbo.2009.05.004
Mertens, K.N., Bradley, L.R., Takano, Y., Mudie, P.J., Marret, F., Aksu, A.E., Hiscott, R.N., Verleye, T.J., Mousing, E.A., Smyrnova, L.L., Bagheri, S., Mansor, M., Pospelova, V., Matsuoka, K., 2012. Quantitative estimation of Holocene surface salinity variation in the Black Sea using dinoflagellate cyst process length. Quaternary Science Reviews 39, 45–59. https://doi.org/10.1016/j.quascirev.2012.01.026
Miehe, G., Miehe, S., Kaiser, K., Reudenbach, C., Behrendes, L., Duo, L., Schlütz, F., 2009. How old is pastoralism in Tibet? An ecological approach to the making of a Tibetan landscape. Palaeogeography, Palaeoclimatology, Palaeoecology 276, 130–147.
Millot, C., 1999. Circulation in the Western Mediterranean Sea. Journal of Marine Systems 20, 423–442. https://doi.org/10.1016/S0924-7963(98)00078-5
Millot, C., 1990. The Gulf of Lions' hydrodynamics. Continental Shelf Research, France-JGOFS, ECOMARGE Particle Fluxes and Ecosystem Response on a Continental Margin 10, 885–894. https://doi.org/10.1016/0278-4343(90)90065-T
Millot, C., 1987. The circulation of the Levantine Intermediate Water in the Algerian Basin. Journal of Geophysical Research: Oceans 92, 8265–8276. https://doi.org/10.1029/JC092iC08p08265

Millot, C., 1985. Some features of the Algerian Current. Journal of Geophysical Research: Oceans 90, 7169–7176. https://doi.org/10.1029/JC090iC04p07169
Millot, C., 1979. Wind induced upwelling in the Gulf of Lions. Oceanologica Acta 2, 261–274.
Millot, C., Taupier-Letage, I., 2005. Circulation in the Mediterranean Sea, in: Saliot, A. (Ed.), The Mediterranean Sea, Handbook of Environmental Chemistry. Springer, Berlin, Heidelberg, pp. 29–66. https://doi.org/10.1007/b107143
Millot, C., Wald, L., 1981. Upwelling in the Gulf of Lions, in: Richards, F.A. (Ed.), Coastal and Estuarine Sciences. American Geophysical Union, Washington, D. C., pp. 160–166. https://doi.org/10.1029/CO001p0160
Miola, A., 2012. Tools for Non-Pollen Palynomorphs (NPPs) analysis: A list of Quaternary NPP types and reference literature in English language (1972–2011). Review of Palaeobotany and Palynology 186, 142–161. https://doi.org/10.1016/j.revpalbo.2012.06.010
Montoya, E., Rull, V., Vegas-Vilarrúbia, T., Corella, J.P., Giralt, S., Valero-Garcés, B., 2018. Grazing activities in the southern central Pyrenees during the last millennium as deduced from the non-pollen palynomorphs (NPP) record of Lake Montcortès. Review of Palaeobotany and Palynology 254, 8–19.
Morán, X.A.G., Taupier-Letage, I., Vázquez-Domínguez, E., Ruiz, S., Arin, L., Raimbault, P., Estrada, M., 2001. Physical-biological coupling in the Algerian Basin (SW Mediterranean): Influence of mesoscale instabilities on the biomass and production of phytoplankton and bacterioplankton. Deep Sea Research Part I: Oceanographic Research Papers 48, 405–437. https://doi.org/10.1016/S0967-0637(00)00042-X
Morel, A., Bricaud, A., André, J.M., Pelaez-Hudlet, J., 1990. Spatial/temporal evolution of the Rhone plume as seen by CZCS imagery-Consequences upon the primary production in the Gulf of Lions. Water Pollution Research Reports 20, 45–62.
Morzadec-Kerfourn, M.T., 1997. Dinoflagellate cysts and the paleoenvironment of Late-Pliocene early-pleistocene deposits of Brittany, Northwest France. Quaternary Science Reviews 16, 883–898.
Morzadec-Kerfourn, M.-T., 1977. La limite Pliocène-Pleistocène en Bretagne. Boreas 6, 275–283.
Moses, T., Kiladis, G.N., Diaz, H.F., Barry, R.G., 1987. Characteristics and frequency of reversals in mean sea level pressure in the North Atlantic sector and their relationship to long-term temperature trends. Journal of Climatology 7, 13–30.
Moutin, T., Raimbault, P., Golterman, H.L., Coste, B., 1998. The input of nutrients by the Rhône river into the Mediterranean Sea: Recent observations and comparison with earlier data, in: Amiard, J.-C., Le Rouzic, B., Berthet, B., Bertru, G. (Eds.), Oceans, Rivers and Lakes: Energy and Substance Transfers at Interfaces, Developments in Hydrobiology. Springer Netherlands, Dordrecht, pp. 237–246. https://doi.org/10.1007/978-94-011-5266-2_19
Moutin, T., Raimbault, P., 2002. Primary production, carbon export and nutrients availability in western and eastern Mediterranean Sea in early summer 1996 (MINOS cruise). Journal of Marine Systems 33, 273–288. https://doi.org/10.1016/S0924-7963(02)00062-3
Najac, J., Boé, J., Terray, L., 2009. A multi-model ensemble approach for assessment of climate change impact on surface winds in France. Clim Dyn 32, 615–634. https://doi.org/10.1007/s00382-008-0440-4
Oguz, T., Macias, D., Garcia-Lafuente, J., Pascual, A., Tintore, J., 2014. Fueling Plankton Production by a Meandering Frontal Jet: A Case Study for the Alboran Sea (Western Mediterranean). PLOS ONE 9, e111482.

https://doi.org/10.1371/journal.pone.0111482
Ozenda, P., P, O., 1975. Sur les étages de la végétation dans les montagnes du bassin méditerranéen., Documentation de cartographie écologique 16, 1–32.
Pande, M., Tarafdar, J.C., 2004. Arbuscular mycorrhizal fungal diversity in neem-based agroforestry systems in Rajasthan. Applied Soil Ecology 26, 233–241.
Papadopoulos, V.P., Josey, S.A., Bartzokas, A., Somot, S., Ruiz, S., Drakopoulou, P., 2012. Large-Scale Atmospheric Circulation Favoring Deep- and Intermediate-Water Formation in the Mediterranean Sea. Journal of Climate 25, 6079–6091. https://doi.org/10.1175/JCLI-D-11-00657.1
Pastor, F., Estrela, M.J., Peñarrocha, D., Millán, M.M., 2001. Torrential Rains on the Spanish Mediterranean Coast: Modeling the Effects of the Sea Surface Temperature. Journal of Applied Meteorology and Climatology 40, 1180–1195. https://doi.org/10.1175/1520-0450(2001)040<1180:TROTSM>2.0.CO;2
Penaud, A., Eynaud, F., Voelker, A.H.L., Turon, J.-L., 2016. Palaeohydrological changes over the last 50 ky in the central Gulf of Cadiz: complex forcing mechanisms mixing multi-scale processes. Biogeosciences 13, 5357–5377.
Penaud, A., Ganne, A., Eynaud, F., Lambert, C., Coste, P.O., Herlédan, M., Vidal, M., Goslin, J., Stéphan, P., Charria, G., Pailler, Y., Durand, M., Zumaque, J., Mojtahid, M., 2020. Oceanic versus continental influences over the last 7 kyrs from a mid-shelf record in the northern Bay of Biscay (NE Atlantic). Quaternary Science Reviews 229, 106135. https://doi.org/10.1016/j.quascirev.2019.106135
Penaud, A., Hardy, W., Lambert, C., Marret, F., Masure, E., Servais, T., Siano, R., Wary, M., Mertens, K.N., 2018. Dinoflagellate fossils: Geological and biological applications. Revue de Micropaléontologie, 60th Anniversary 61, 235–254. https://doi.org/10.1016/j.revmic.2018.09.003
Perkins, H., Pistek, P., 1990. Circulation in the Algerian Basin during June 1986. Journal of Geophysical Research: Oceans 95, 1577–1585. https://doi.org/10.1029/JC095iC02p01577
Polunin, O., Walters, M., 1985. guide to the vegetation of Britain and Europe. Oxford University Press.
Pospelova, V., Chmura, G.L., Boothman, W.S., Latimer, J.S., 2005. Spatial distribution of modern dinoflagellate cysts in polluted estuarine sediments from Buzzards Bay (Massachusetts, USA) embayments. Marine Ecology Progress Series 292, 23–40. https://doi.org/10.3354/meps292023
Pospelova, V., Chmura, G.L., Walker, H.A., 2004. Environmental factors influencing the spatial distribution of dinoflagellate cyst assemblages in shallow lagoons of southern New England (USA). Review of Palaeobotany and Palynology, Middle latitude dinoflagellates and their cysts 128, 7–34. https://doi.org/10.1016/S0034-6667(03)00110-6
Pospelova, V., de Vernal, A., Pedersen, T.F., 2008. Distribution of dinoflagellate cysts in surface sediments from the northeastern Pacific Ocean (43–25°N) in relation to sea-surface temperature, salinity, productivity and coastal upwelling. Marine Micropaleontology, Dinocysts as tracers of hydrographical conditions and productivity along the ocean margins 68, 21–48. https://doi.org/10.1016/j.marmicro.2008.01.008
Prospero, J.M., 1996. Saharan Dust Transport Over the North Atlantic Ocean and Mediterranean: An Overview, in: Guerzoni, S., Chester, R. (Eds.), The Impact of Desert Dust Across the Mediterranean, Environmental Science and Technology Library. Springer Netherlands, Dordrecht, pp. 133–151. https://doi.org/10.1007/978-94-017-3354-0_13

Quézel, P., Médail, F., 2003. Que faut-il entendre par' forêts méditerranéennes. Forêt méditerranéenne 24, 11–31.
Radi, T., Pospelova, V., de Vernal, A., Vaughn Barrie, J., 2007. Dinoflagellate cysts as indicators of water quality and productivity in British Columbia estuarine environments. Marine Micropaleontology 62, 269–297. https://doi.org/10.1016/j.marmicro.2006.09.002
Raghukumar, C., Nagarkar, S., Raghukumar, S., 1992. Association of thraustochytrids and fungi with living marine algae. Mycological Research 96, 542–546.
Raimbault, P., Coste, B., Boulhadid, M., Boudjellal, B., 1993. Origin of high phytoplankton concentration in deep chlorophyll maximum (DCM) in a frontal region of the Southwestern Mediterranean Sea (Algerian Current). Deep Sea Research Part I: Oceanographic Research Papers 40, 791–804.
Reid, P.C., 1975. A regional sub-division of dinoflagellate cysts around the British Isles. New Phytologist 75, 589–603.
Reille, M., 1992. Pollen et spores d'Europe et d'Afrique du Nord. Laboratoire de Botanique historique et Palynologie.
Rivas-Martinez, S., 1982. Etages bioclimatiques, secteurs chorologiques et séries de végétation de l'Espagne méditerranéenne. Ecologia Mediterranea 8, 275–288. https://doi.org/10.3406/ecmed.1982.1954
Rochon, A., Vernal, A. de, Turon, J.-L., Matthießen, J., Head, M.J., 1999. Distribution of recent dinoflagellate cysts in surface sediments from the North Atlantic Ocean and adjacent seas in relation to sea-surface parameters. American Association of Stratigraphic Palynologists Contribution Series 35, 1–146.
Rohling, E.J., Abu-Zied, R., Casford, J.S.L., Hayes, A., Hoogakker, B.A.A., 2009. The marine environment: present and past. The physical geography of the Mediterranean 33–67.
Rohling, E.J., Den Dulk, M., Pujol, C., Vergnaud-Grazzini, C., 1995. Abrupt hydrographic change in the Alboran Sea (western Mediterranean) around 8000 yrs BP. Deep Sea Research Part I: Oceanographic Research Papers 42, 1609–1619.
Schmidt, S., Tronczyński, J., Guiot, N., Lefevre, I., 2005. Dating of sediments in the Biscay bay: Implication for pollution chronology. http://dx.doi.org/10.1051/radiopro:2005s1-096 40. https://doi.org/10.1051/radiopro:2005s1-096
Schwarzott, D., Walker, C., Schüßler, A., 2001. Glomus, the largest genus of the arbuscular mycorrhizal fungi (Glomales), is nonmonophyletic. Molecular Phylogenetics and Evolution 21, 190–197.
Shumilovskikh, L., O'Keefe, J.M., Marret, F., 2021. An overview of the taxonomic groups of NPPs. Geological Society, London, Special Publications 511.
Shumilovskikh, L.S., Hopper, K., Djamali, M., Ponel, P., Demory, F., Rostek, F., Tachikawa, K., Bittmann, F., Golyeva, A., Guibal, F., Talon, B., Wang, L.-C., Nezamabadi, M., Bard, E., Lahijani, H., Nokandeh, J., Omrani Rekavandi, H., de Beaulieu, J.-L., Sauer, E., Andrieu-Ponel, V., 2016. Landscape evolution and agro-sylvo-pastoral activities on the Gorgan Plain (NE Iran) in the last 6000 years. The Holocene 26, 1676–1691. https://doi.org/10.1177/0959683616646841
Skliris, N., Sofianos, S., Gkanasos, A., Mantziafou, A., Vervatis, V., Axaopoulos, P., Lascaratos, A., 2012. Decadal scale variability of sea surface temperature in the Mediterranean Sea in relation to atmospheric variability. Ocean Dynamics 62, 13–30. https://doi.org/10.1007/s10236-011-0493-5
Skliris, N., Zika, J.D., Herold, L., Josey, S.A., Marsh, R., 2018. Mediterranean sea water budget long-term trend inferred from salinity observations. Clim Dyn 51, 2857–2876. https://doi.org/10.1007/s00382-017-4053-7

Sournia, A., 1973. La production primaire planctonique en Méditerranée, essai de mise à jour. LA PRODUCTION PRIMAIRE PLANCTONIQUE EN MEDITERRANEE. ESSAI DE MISE A JOUR.
Stockmarr, J.A., 1971. Tabletes with spores used in absolute pollen analysis. Pollen spores 13, 615–621.
Stürmer, S.L., Bever, J.D., Morton, J.B., 2018a. Biogeography of arbuscular mycorrhizal fungi (Glomeromycota): a phylogenetic perspective on species distribution patterns. Mycorrhiza 28, 587–603.
Stürmer, S.L., Oliveira, L.Z., Morton, J.B., 2018b. Gigasporaceae versus Glomeraceae (phylum Glomeromycota): a biogeographic tale of dominance in maritime sand dunes. Fungal Ecology 32, 49–56.
Stutz, J.C., Copeman, R., Martin, C.A., Morton, J.B., 2000. Patterns of species composition and distribution of arbuscular mycorrhizal fungi in arid regions of southwestern North America and Namibia, Africa. Canadian Journal of Botany 78, 237–245.
Suc, J.P., 1989. Distribution latitudinale et etagement des associations vegetales au Cenozoique superieur dans l'aire ouest-mediterraneenne. Bulletin de la Société Géologique de France V, 541–550. https://doi.org/10.2113/gssgfbull.V.3.541
Targarona, J., Warnaar, J., Boessenkool, K.P., Brinkhuis, H., Canals, M., 1999. Recent dinoflagellate cyst distribution in the North Canary Basin, NW Africa. Grana 38, 170–178.
Taupier-Letage, I., Puillat, I., Millot, C., Raimbault, P., 2003. Biological response to mesoscale eddies in the Algerian Basin. Journal of Geophysical Research: Oceans 108, 32–45. https://doi.org/10.1029/1999JC000117
Thornes, J.B., 2002. The evolving context of Mediterranean desertification. Mediterranean Desertification: A Mosaic of Processes and Responses 5–11.
Tintore, J., Violette, P.E.L., Blade, I., Cruzado, A., 1988. A Study of an Intense Density Front in the Eastern Alboran Sea: The Almeria–Oran Front. Journal of Physical Oceanography 18, 1384–1397. https://doi.org/10.1175/1520-0485(1988)018<1384:ASOAID>2.0.CO;2
Tsimplis, M.N., Zervakis, V., Josey, S.A., Peneva, E.L., Struglia, M.V., Stanev, E.V., Theocharis, A., Lionello, P., Malanotte-Rizzoli, P., Artale, V., Tragou, E., Oguz, T., 2006. Chapter 4 Changes in the oceanography of the Mediterranean Sea and their link to climate variability, in: Lionello, P., Malanotte-Rizzoli, P., Boscolo, R. (Eds.), Developments in Earth and Environmental Sciences, Mediterranean. Elsevier, pp. 227–282. https://doi.org/10.1016/S1571-9197(06)80007-8
Turon, J.-L., 1984. Direct land/sea correlations in the last interglacial complex. Nature 309, 673–676.
Tzoraki, O., Nikolaidis, N.P., 2007. A generalized framework for modeling the hydrologic and biogeochemical response of a Mediterranean temporary river basin. Journal of Hydrology 346, 112–121. https://doi.org/10.1016/j.jhydrol.2007.08.025
van Geel, B., 1978. A palaeoecological study of holocene peat bog sections in Germany and The Netherlands, based on the analysis of pollen, spores and macro- and microscopic remains of fungi, algae, cormophytes and animals. Review of Palaeobotany and Palynology 25, 1–120. https://doi.org/10.1016/0034-6667(78)90040-4
van Geel, B., Buurman, J., Brinkkemper, O., Schelvis, J., Aptroot, A., van Reenen, G.B.A., Hakbijl, T., 2003. Environmental reconstruction of a Roman Period settlement site in Uitgeest (The Netherlands), with special reference to coprophilous fungi. Journal of Archaeological Science 30. https://doi.org/10.1016/S0305-4403(02)00265-0
van Geel, B., Coope, G., Hammen, T., 1989. Palaeocology and stratigraphy of the Lateglacial type section at Usselo (The Netherlands). Review of Palaeobotany and Palynology 60,

25–129. https://doi.org/10.1016/0034-6667(89)90072-9
van Geel, B., Hallewas, D.P., Pals, J.P., 1983. A late Holocene deposit under the Westfriese Zeedijk near Enkhuizen (Prov. of Noord-Holland, The Netherlands): Palaeoecological and archaeological aspects. Review of Palaeobotany and Palynology 38, 269–335. https://doi.org/10.1016/0034-6667(83)90026-X
Van Geel, B., Aptroot, A., 2006. Fossil ascomycetes in Quaternary deposits. Nova Hedwigia 82, 313–329. https://doi.org/10.1127/0029-5035/2006/0082-0313
Van Nieuwenhove, N., Pospelova, V., Anne, de V., Rochon, A., 2020. A historical perspective on the development of the Northern Hemisphere modern dinoflagellate cyst database. Marine Micropaleontology 159, 101824. https://doi.org/10.1016/j.marmicro.2020.101824
Vernal, A. de, Henry, M., Matthiessen, J., Mudie, P.J., Rochon, A., Boessenkool, K.P., Eynaud, F., GrØsfjeld, K., Guiot, J., Hamel, D., Harland, R., Head, M.J., Kunz-Pirrung, M., Levac, E., Loucheur, V., Peyron, O., Pospelova, V., Radi, T., Turon, J.-L., Voronina, E., 2001. Dinoflagellate cyst assemblages as tracers of sea-surface conditions in the northern North Atlantic, Arctic and sub-Arctic seas: the new 'n = 677' data base and its application for quantitative palaeoceanographic reconstruction. Journal of Quaternary Science 16, 681–698. https://doi.org/10.1002/jqs.659
Violette, P.E.L., 1986. Short-term Measurements of Surface Currents Associated with the Alboran Sea Gyre during Donde Va? Journal of Physical Oceanography 16, 262–279. https://doi.org/10.1175/1520-0485(1986)016<0262:STMOSC>2.0.CO;2
Viúdez, Á., Tintoré, J., 1995. Time and space variability in the eastern Alboran Sea from March to May 1990. Journal of Geophysical Research: Oceans 100, 8571–8586.
Wall, D., Dale, B., Lohmann, G.P., Smith, W.K., 1977. The environmental and climatic distribution of dinoflagellate cysts in modern marine sediments from regions in the North and South Atlantic Oceans and adjacent seas. Marine micropaleontology 2, 121–200.
Wang, Z., Matsuoka, K., Qi, Y., Chen, J., 2004. Dinoflagellate Cysts in Recent Sediments from Chinese Coastal Waters. Marine Ecology 25, 289–311. https://doi.org/10.1111/j.1439-0485.2004.00035.x
Xin, C., Zhi-Guo, F., Jian-Jun, T., 2001. Investigation on host plants of vesicular arbuscular mycorrhiza fungi (VAMF) wi thin weed communities in agricultural slope land in the red soil area of southea stern Chi na. Biodiversity Science 9, 122.
Yebra, L., Herrera, I., Mercado, J.M., Cortés, D., Gómez-Jakobsen, F., Alonso, A., Sánchez, A., Salles, S., Valcárcel-Pérez, N., 2018. Zooplankton production and carbon export flux in the western Alboran Sea gyre (SW Mediterranean). Progress in Oceanography 167, 64–77. https://doi.org/10.1016/j.pocean.2018.07.009
Zhao, Y.-Y., Morzadec-Kerfourn, M.-T., 1992. Kystes de Dinoflagellés, pollens et spores des sédiments quaternaires du Bassin abyssal de Mer de Chine du Sud: leur signification paléoenvironnementale. Revue de Micropaléontologie 35, 77–88.
Zonneveld, K.A., Ganssen, G., Troelstra, S., Versteegh, G.J., Visscher, H., 1997. Mechanisms forcing abrupt fluctuations of the Indian Ocean summer monsoon during the last deglaciation. Quaternary Science Reviews 16, 187–201.
Zonneveld, K.A.F., Chen, L., Möbius, J., Mahmoud, M.S., 2009. Environmental significance of dinoflagellate cysts from the proximal part of the Po-river discharge plume (off southern Italy, Eastern Mediterranean). Journal of Sea Research 62, 189–213. https://doi.org/10.1016/j.seares.2009.02.003
Zonneveld, K.A.F., Marret, F., Versteegh, G.J.M., Bogus, K., Bonnet, S., Bouimetarhan, I., Crouch, E., de Vernal, A., Elshanawany, R., Edwards, L., Esper, O., Forke, S., Grøsfjeld, K., Henry, M., Holzwarth, U., Kielt, J.-F., Kim, S.-Y., Ladouceur, S., Ledu,

D., Chen, L., Limoges, A., Londeix, L., Lu, S.-H., Mahmoud, M.S., Marino, G., Matsouka, K., Matthiessen, J., Mildenhal, D.C., Mudie, P., Neil, H.L., Pospelova, V., Qi, Y., Radi, T., Richerol, T., Rochon, A., Sangiorgi, F., Solignac, S., Turon, J.-L., Verleye, T., Wang, Y., Wang, Z., Young, M., 2013. Atlas of modern dinoflagellate cyst distribution based on 2405 data points. Review of Palaeobotany and Palynology, Atlas of modern dinoflagellate cyst distribution based on 2405 data points 191, 1–197. https://doi.org/10.1016/j.revpalbo.2012.08.003

Table 1

Cruise	Year	Core	OBS (cm)	Latitude (°N)	Longitude (°E)	Depth (m)	Lithology	Age range	Reference of dating
PRISME	2007	PSM-KS19	0–1.5	36.63	0.29	2624	Mud	60 < T < 100 yrs	this study
PRISME	2007	PSM-KS20	0–1	36.80	0.62	2652	Mud	100 < T < 200 yrs	this study
PRISME	2007	PSM-KS30	0–1	37.19	3.34	2769	Mud	No date	
PRISME	2007	PSM-KS33	0–1	36.80	3.50	104	Sandy mud	T < 60 yrs	this study
PRISME	2007	PSM-KS34	0.5–2	36.82	3.54	137	Sandy mud	T < 60 yrs	this study
PRISME	2007	PSM-KS35	0–1	36.81	3.49	131	Sandy mud	T < 60 yrs	this study
MARADJA	2003	IMDJ03	0–0.5	36.95	3.29	2431	Mud	No date	
MARADJA2	2005	IMDJ12	0–1	37.00	3.79	1650	Mud	No date	
MARADJA2	2005	IMDJ25	0–0.5	36.46	0.42	2354	Mud	30 < T < 60 yrs	this study
MARADJA	2003	KMDJ07	0–1	36.54	0.13	2624	Mud	100 < T < 200 yrs	this study
MARADJA2	2005	KMDJ13	0–1	37.03	3.77	2158	Mud	No date	
MARADJA2	2005	KMDJ19	0–0.5	36.96	3.19	2473	Mud	60 < T < 100 yrs	Genet (2022)
MARADJA2	2005	KMDJ20	0–0.5	36.98	3.33	2343	Mud	100 < T < 200 yrs	Genet (2022)
MARADJA2	2005	KMDJ22	0–0.5	36.48	0.47	2098	Mud	30 < T < 60 yrs	this study
MARADJA2	2005	KMDJ23	0–0.5	36.50	0.26	2542	Mud	30 < T < 60 yrs	this study
MARADJA2	2005	KMDJ24	0–0.5	36.47	0.42	2354	Mud	30 < T < 60 yrs	this study
MARADJA2	2005	KMDJ29	0–0.5	36.91	2.67	616	Mud	No date	
MARADJA2	2005	KMDJ36	0–1	37.13	5.36	2462	Mud	No date	
MARADJA2	2005	KMDJ38	0–1	37.22	8.00	1015	Mud	T < 60 yrs	this study
GMO2-CARNAC	2002	KIGC 01	0–0.5	41.92	4.71	2435	Mud	T < 20 yrs	Genet (2022)
BEACHMED	2004	BM-KS12	0–0.5	43.44	4.02	29	Mud	60 < T < 100 yrs	Genet (2022)
RHOSOS	2008	RHS-KS39	0–0.5	43.38	4.51	20	Sandy mud	20 < T < 60 yrs	Genet (2022)
RHOSOS	2008	RHS-KS51	0–0.5	43.27	4,92	89	Sandy mud	20 < T < 60 yrs	Genet (2022)
GMO1	2001	KGMO-10	0–0.5	42.26	4.78	2066	Mud	T < 20 yrs	Genet (2022)
GMO1	2001	KGMO-14	0–0.5	42.78	3.67	234	Sand	100 < T < 200 yrs	Genet (2022)

Figure 1

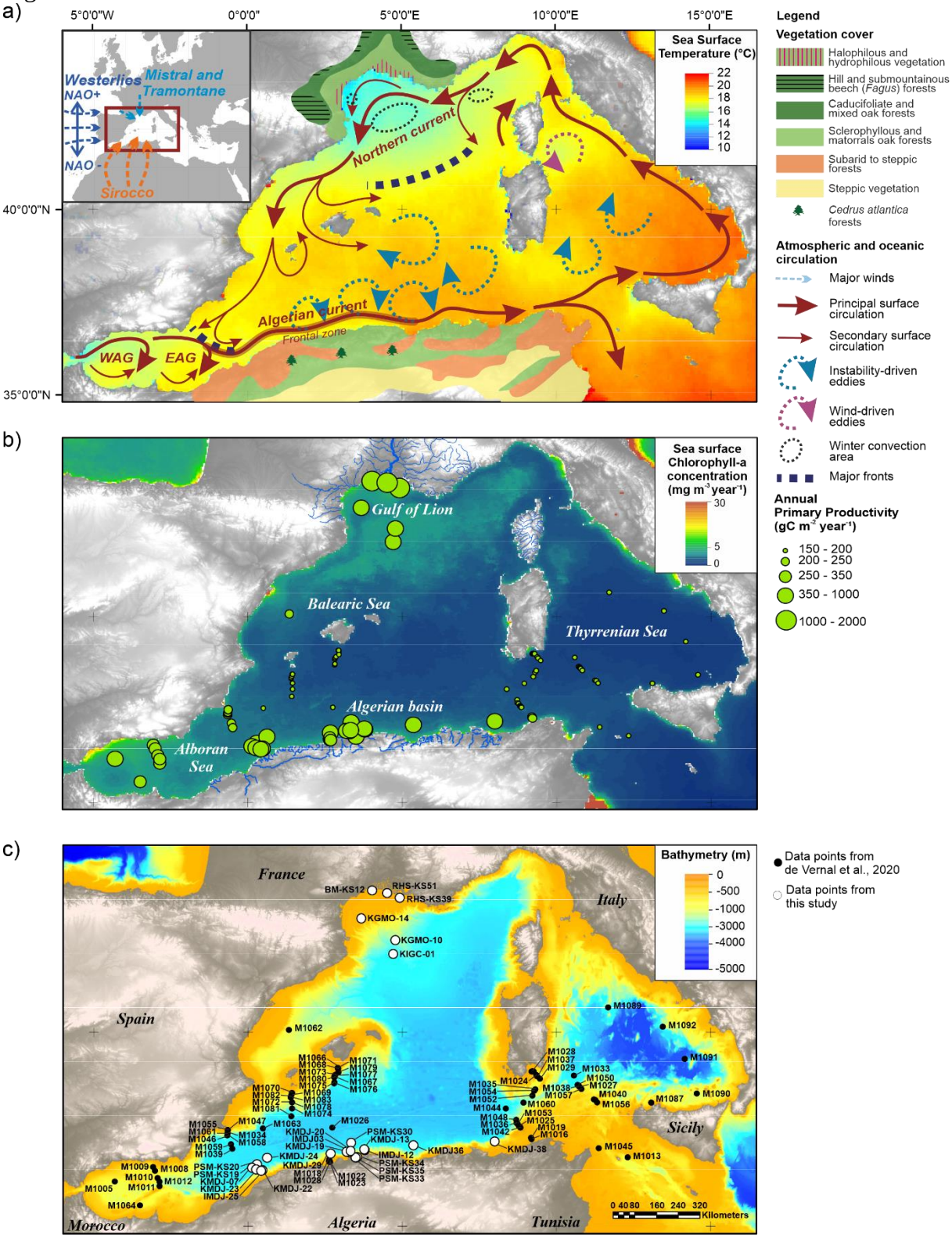
a)
5°0'0"W
0°0'0"
5°0'0"E
10°0'0"E
15°0'0"E
40°0'0"N
35°0'0"N
Westerlies
NAO+
Mistral and Tramontane
NAO-
Sirocco
Northern current
Algerian current
Frontal zone
WAG
EAG
Sea Surface Temperature (°C)
22
20
18
16
14
12
10
Legend
Vegetation cover
Halophilous and hydrophilous vegetation
Hill and submountainous beech (Fagus) forests
Caducifoliate and mixed oak forests
Sclerophyllous and matorrals oak forests
Subarid to steppic forests
Steppic vegetation
Cedrus atlantica forests
Atmospheric and oceanic circulation
Major winds
Principal surface circulation
Secondary surface circulation
Instability-driven eddies
Wind-driven eddies
Winter convection area
Major fronts
b)
Gulf of Lion
Balearic Sea
Thyrrenian Sea
Algerian basin
Alboran Sea
Sea surface Chlorophyll-a concentration (mg m-3 year-1)
30
5
0
Annual Primary Productivity (gC m-2 year-1)
150 - 200
200 - 250
250 - 350
350 - 1000
1000 - 2000
c)
France
Italy
Spain
Sicily
Morocco
Algeria
Tunisia
Bathymetry (m)
0
-500
-1000
-3000
-4000
-5000
BM-KS12
RHS-KS51
RHS-KS39
KGMO-14
KGMO-10
KIGC-01
PSM-KS30
KMDJ-13
KMDJ-19
KMDJ-20
KMDJ-24
KMDJ-29
KMDJ-22
KMDJ-12
KMDJ36
KMDJ-38
PSM-KS34
PSM-KS35
PSM-KS33
PSM-KS20
PSM-KS19
KMDJ-07
KMDJ-23
IMDJ-25
0 40 80 160 240 320
Kilometers
Data points from de Vernal et al., 2020
Data points from this study

Figure2

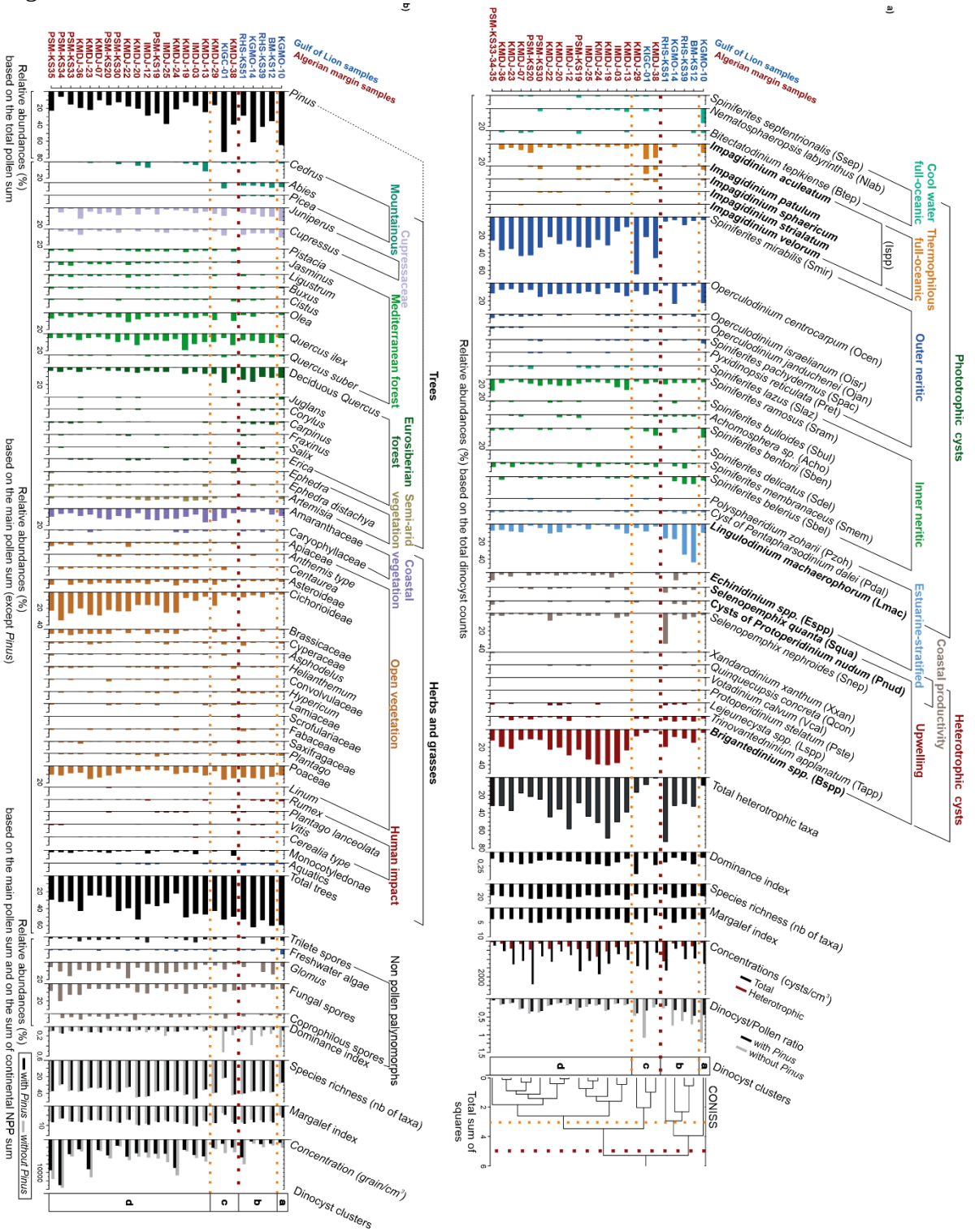

Figure 3

a) Dinocyst data

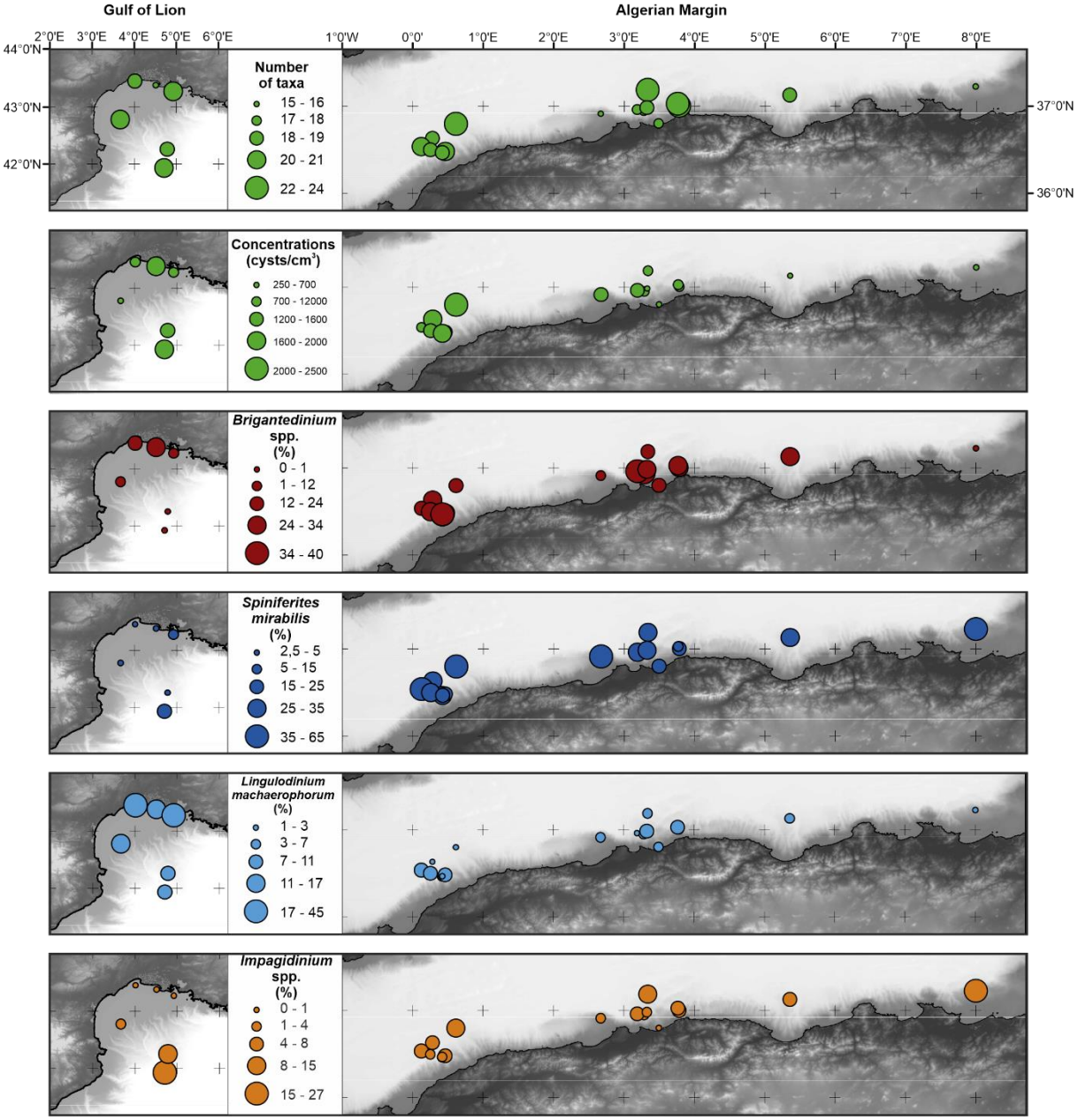

b) Pollen data

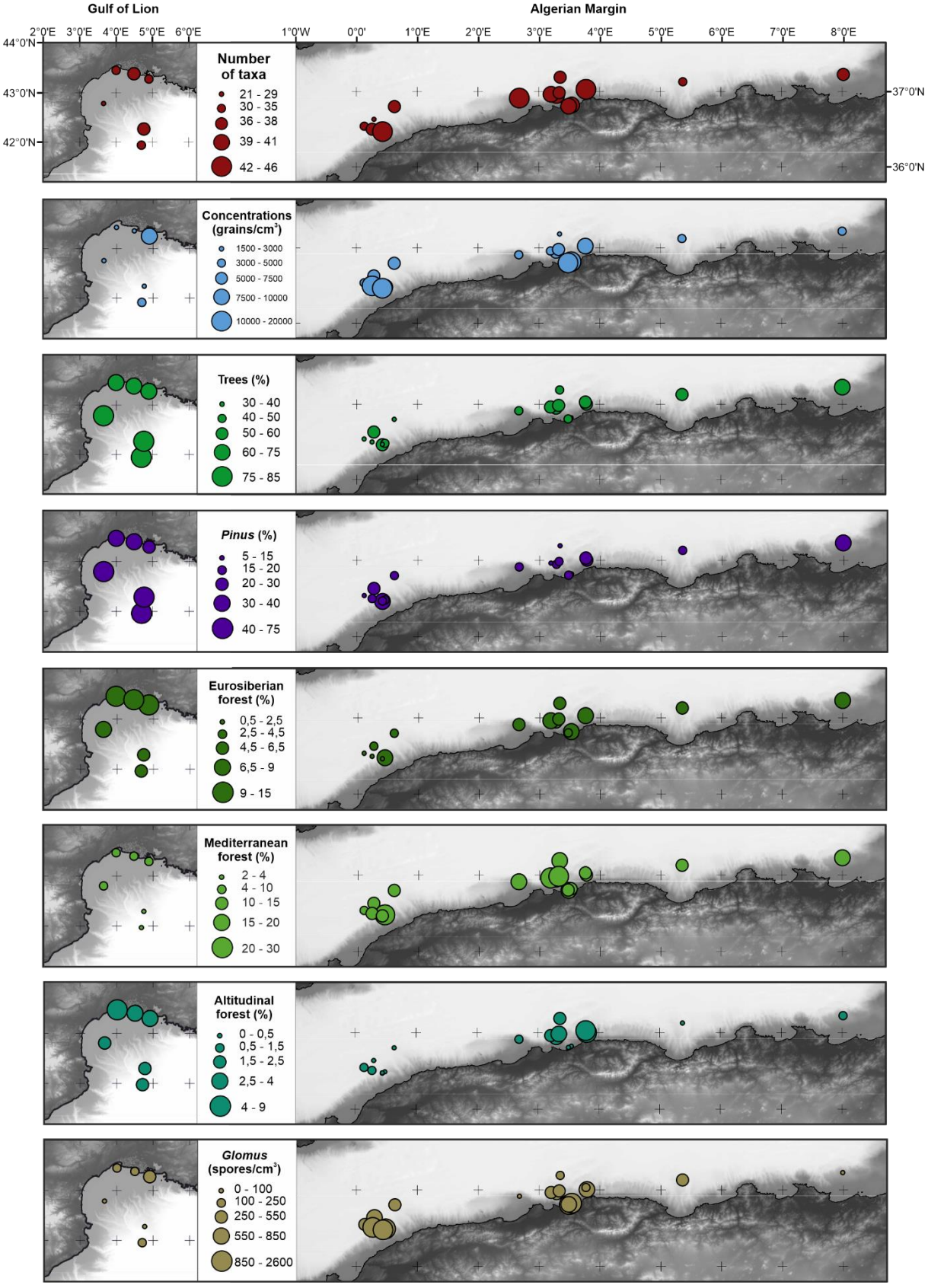

Figure 4

Figure 5

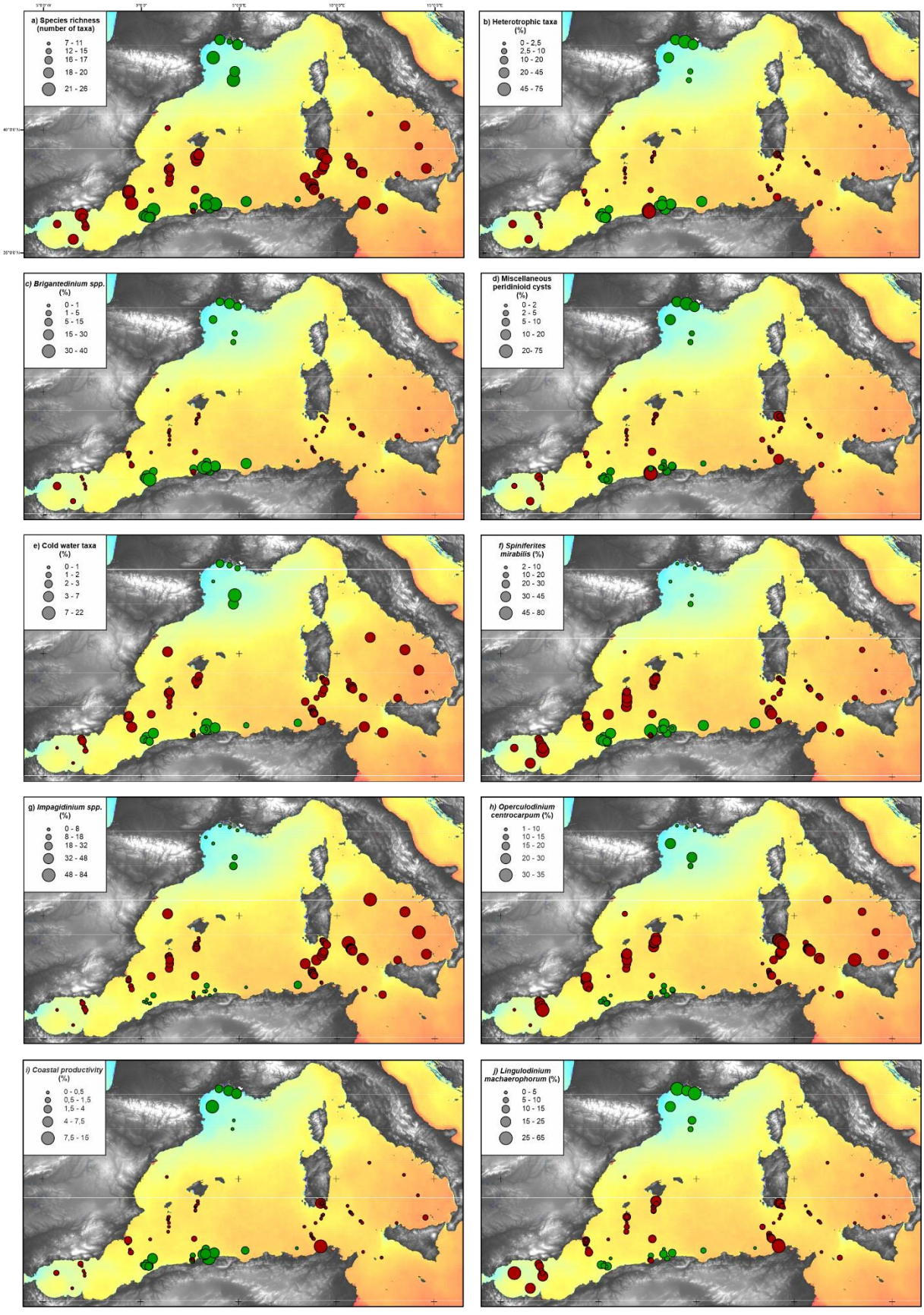
a) Species richness (number of taxa)
7 - 11
12 - 15
16 - 17
18 - 20
21 - 26
b) Heterotrophic taxa (%)
0 - 2,5
2,5 - 10
10 - 20
20 - 45
45 - 75
c) Brigantedinium spp. (%)
0 - 1
1 - 5
5 - 15
15 - 30
30 - 40
d) Miscellaneous peridinioid cysts (%)
0 - 2
2 - 5
5 - 10
10 - 20
20- 75
e) Cold water taxa (%)
0 - 1
1 - 2
2 - 3
3 - 7
7 - 22
f) Spiniferites mirabilis (%)
2 - 10
10 - 20
20 - 30
30 - 45
45 - 80
g) Impagidinium spp. (%)
0 - 8
8 - 18
18 - 32
32 - 48
48 - 84
h) Operculodinium centrocarpum (%)
1 - 10
10 - 15
15 - 20
20 - 30
30 - 35
i) Coastal productivity (%)
0 - 0,5
0,5 - 1,5
1,5 - 4
4 - 7,5
7,5 - 15
j) Lingulodinium machaerophorum (%)
0 - 5
5 - 10
10 - 15
15 - 25
25 - 65

Figure 6

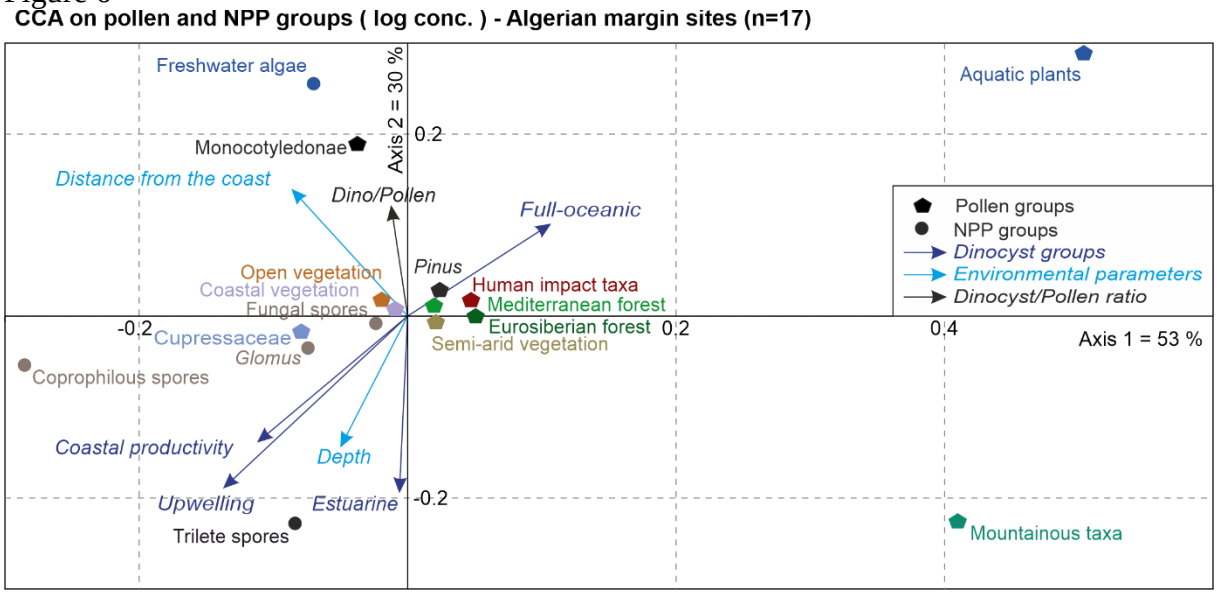

Figure 7